Master Thesis

Influence of the sugars present in grass silage model solution on lactic acid recovery through nanofiltration process

Carried out for the purpose of obtaining the degree of Master of Science

Diplom-Ingenieur

By

Khaled Maamo

Matr. Nr. 11811857

Under the supervision of

Ao. Univ.Prof. Dipl.-Ing. Dr.techn. Michael Harasek[1]

Projektass. Dr.Amal El Gohary Ahmed[1]

PH.D. researcher Mayuki Cabrera-González[1]

Univ.Ass. Dipl.-Ing. Dr.techn. Christian Jordan[1]

[1]E166 Institute of Chemical, Environmental and Bioscience Engineering

Submitted at Vienna University of Technology

Faculty of Mechanical and Industrial Engineering

Vienna, January 2022

Khaled Maamo

TECHNISCHE UNIVERSITÄT WIEN

I confirm that going to press of this thesis needs the confirmation of the examination committee.

Affidavit

In lieu of oath, I declare that I wrote this thesis and performed the associated research myself, using only literature cited in this volume. If text passages from sources are used literally, they are marked as such.

I confirm that this work is original and has not been submitted elsewhere for any examination, nor is it currently under consideration for a thesis elsewhere

Vienna, January 2022

Khaled Maamo

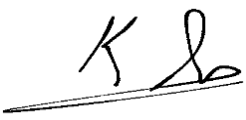

Acknowledgments

I would like to express my deepest gratitude to my supervisor Ao. Univ.Prof. Dipl.-Ing. Dr.techn. **Michael Harasek** for giving me the chance to work on this project. I will always keep aspiring to his level of patience, knowledge, and ingenuity.

This work would not have been possible without the constant support, guidance, and assistance of senior researcher. Dr.**Amal El Gohary Ahmed .** No words can describe her brilliant, skillful supervision; thank you from the depth of my heart.

My sincere thanks also go to Dipl.-Ing. Dr.techn.**Christian Jordan** and Ph.D. researcher **Mayuki Cabrera-González** for their generous participation in guiding, constructive feedback, kind support, and advice.

Special thanks to my committee members Ao. Univ. Prof. Dipl.-Ing. Dr.techn.**Andreas Werner** and Ao. Univ. Prof. Dipl.- Ing. Dr.techn.**Franz Winter.**

I am highly thankful to Dipl.-Ing. Dr.techn.**Stefan Beisl**, and Univ.Ass. Dipl.-Ing. **Johannes Adamcyk** for assisting me with operating HPLC system.

Thank is also extended to all Chemical, Environmental, and Bioscience Engineering Institute members.

Dear **Mohammad Salem**, it was a pleasure to work with you. Your kindness, generosity, and dedication to work have teched me a lot. Thank you my brother

To my mother,my love that will remain forever. Thank you for being my mother, and sorry that I didn´t find the words you deserve. **M**ama, it´s all thanks to you

to my role model, my dear father thank you for everything you have given me … I love you

to my beloved sister, thank you for the financial support.

thank you (**Pella**) for becoming a new member of our family, wishing you all success in learning to walk next year.

(Fares) you were always with me.your soul, smile, and eyes guided me in the most challenging moments. I dedicate this work to your pure soul.

Tabel of Contents

Abstract

With growing worries about environmental safety, fast economic development, finite fossil fuel reserves, and fluctuating oil prices, the interest in producing fuel and industrial chemicals from renewable resources and biomass is expanding. The biomass feedstock is converted into biofuels, and bio-based chemicals like lactic acid (LA), in a biorefinery.

LA has been widely utilized in the food, cosmetic, and pharmaceutical industries. LA is manufactured either by biomass fermentation or chemical synthesis. The fermentation process is attractive because of its advantages of using renewable carbohydrates and producing optically pure LA. However, the primary challenge associated with bio-based lactic acid production is the presence of impurities like glucose, fructose, salts, and other organic acids. Membrane technology has been established for lactic acid purification from those impurities.

The optimization of lactic acid recovery from the grass silage model solution using the nanofiltration membrane process was investigated. In addition, the effect of residual glucose and fructose in this silage model solution was studied. Four commercial nanofiltrations (NF) membranes (Alfa Laval, NF-Toray, NF 270, and SELRO MPF-36) were tested at different operating conditions of temperature and pH. All experiments were conducted in a lab-scale membrane unit. The performance of each membrane regarding the rejection of lactic acid, Acetic acid, and sugars was measured.

Alfa Laval achieved the highest lactic acid recovery at room temperature and pH around 2,8. Glucose and fructose have different impacts on the rejection of LA; this effect can be positive or negative depending on the membrane material and Molecular weight cut-off (MWCO). In general, the presence of fructose in the model solution decreases the LA rejection, and in contrast, glucose has a negative effect as it increases LA rejection.

Zusammenfassung

Angesichts der zunehmenden Sorge um die Umweltsicherheit, das rasante wirtschaftliche Entwicklung, die endliche Reserven fossiler Brennstoffe und die schwankenden Ölpreise wächst das Interesse an der Herstellung von Kraftstoffen und Industriechemikalien aus erneuerbaren Ressourcen und Biomasse. Der Biomasse-Rohstoff wird in einer Bioraffinerie in Biokraftstoffe und biobasierte Chemikalien wie Milchsäure (LA) umgewandelt.

Milchsäure wird in der Lebensmittel-, Kosmetik- und Pharmaindustrie in großem Umfang eingesetzt. LA wird entweder durch Fermentation von Biomasse oder durch chemische Synthese hergestellt. Das Fermentationsverfahren ist attraktiv, da es die Vorteile der Verwendung erneuerbarer Kohlenhydrate und der Herstellung optisch reiner Milchsäure bietet. Die größte Herausforderung bei der biobasierten Milchsäureproduktion ist jedoch das Vorhandensein von Verunreinigungen wie Glukose, Fruktose, Salzen und anderen organischen Säuren. Für die Rückgewinnung der Milchsäure aus diesen Verunreinigungen hat sich die Membrantechnologie etabliert.

Die Optimierung der Milchsäuregewinnung aus der Grassilage-Modelllösung unter Verwendung des Nanofiltrationsmembranverfahrens wurde untersucht. Darüber hinaus wurde die Auswirkung von Restglukose und -fruktose in dieser Silage-Modelllösung untersucht. Vier kommerzielle Nonofiltrations (NF) -Membranen (Alfa Laval, NF-Toray, NF 270 und SELRO MPF-36) wurden bei unterschiedlichen Betriebsbedingungen (Temperatur und pH-Wert) getestet. Alle Versuche wurden in einer Membrananlage im Labormaßstab durchgeführt. Die Leistung der einzelnen Membranen in Bezug auf das Ausschlussrate von Milchsäure, Essigsäure und Zuckern wurde gemessen.

Alfa Laval erreicht die höchste LA-Gewinnung bei Raumtemperatur und einem pH-Wert um 2,8. Glukose und Fruktose haben unterschiedliche Auswirkungen auf die Ausschussrate von LA; dieser Effekt kann je nach Membranmaterial und MWCO (Molecular weight cut-off) positiv oder negativ sein. Im Allgemeinen verringert das Vorhandensein von Fruktose in der Modelllösung die LA-Abstoßung, während Glukose einen negativen Effekt hat, da sie die LA-Abstoßung erhöht.

List of Tables

List of Figures

Abbreviation

WMO	World Meteorological Organization
GHG	Greenhouse gases
LA	Lactic acid
CAGR	Compound annual growth rate
AA	Acetic acid
LCB	Lignocellulosic biomass
LAB	Lactic acid Bacteria
DM	Dry matter
ED	Electro dialysis
UF	Ultrafiltration
MF	Microfiltration
NF	Nanofiltration
RO	Reverse osmosis
MWCO	Molecular weight cut-off
CSTR	Continuous Stirred Tank Reactors
DM	Dry matter
NDF	Neutral detergent fiber
CP	Concentration polarization
OPD	Osmotic pressure difference
CECP	Cake-enhanced concentration polarization
DSPM	Donnan-Steric-Pore model
EMP	Embden–Meyerhof–Parnas
GLU	Glucose
FRU	Fructose

List of Symbols

J	Flux	[$m^3.m^{-2}.s^{-1}$]
J s	Solute flux	[$m^3.m^{-2}.s^{-1}$]
J v	Solvent flux	[$m^3.m^{-2}.s^{-1}$]
M	Total mass transferred membrane area	[Kg]
D	Diffusion coefficient	[$m^2.s^{-1}$]
$D_{i,p}$	Pore diffusion coefficient	[$m^2.s^{-1}$]
$D_{i\infty}$	The diffusion coefficient in Bulk	[$m^2.s^{-1}$]
S_{ij}	Membrane selectivity	-
y_i , y_j	Mole fraction for components i,j in permeate	-
x_i , x_j	Mole fraction for components i,j in feed	-
R	Rejection	[%]
$C_{P,i}$	The permeate concentration of the species i	[mole $.m^{-3}$]
$C_{R,i}$	The retentate concentration of the species i	[mole $.m^{-3}$]
C_f	Concentration of Solute in feed	[mole $.m^{-3}$]
C_b	Concentrations of solute in bulk	[mole $.m^{-3}$]
C_W	Concentrations of solute at the membrane surface	[mole $.m^{-3}$]
δ	Membrane thickness	[m]
k	Mass transfer coefficient	[$m.s^{-1}$]
TMP	Transmembrane pressure	[bar]
$\Delta\pi i$	Osmotic pressure difference across the membrane	[bar]
Rm	Intrinsic membrane resistance	[$Kg.m^{-2}. s^{-1}$]
Rf	Total fouling resistance	[$Kg.m^{-2}. s^{-1}$]
L_P	Membrane's hydraulic permeability	[$m^3.m^{-2}.s^{-1}.bar^{-1}$]
σ	Reflection coefficient	-
μ_i	Chemical potential	[J. mol^{-1}]
$K_{i,c}$	Convective hindrance factor	-
$K_{i,d}$	Diffusive hindrance factor	-
R_g	Ideal gas constant	8,314 [$Jmol^{-1} .K^{-1}$]
a_i	The activity coefficient of ion i	-
V_{si}	The specific volume of ion i	[$m^3.Kg^{-1}$]

z_{i}	The valence of ion i	-
F	Faraday constant	96,485 [C.mol^{-1}]
ψ	Electrical potential in the membrane	[V]
$\Delta\psi_{\mathrm{D}}$	Donnan potential difference	[V]
γ_i	Activity coefficient	-
u	Solvent velocity	[m.s^{-1}]
φ_{i}	The steric partition coefficient of solute i	-
r_{i}	Solute radius i	[m]
r_{p}	Pore radius	[m]
η	The viscosity inside the pore	[pa.s]
η_0	The bulk solvent viscosity	[pa.s]
Pe	Peclet number	-
$g(\rho)$	The radial distribution function	-
ϕ	The partition coefficient	-
K_b	Boltzmann constant	1,38066 . 10^{-23} [J.K^{-1}]
ΔG_i	The free-energy difference	[KJ. mol^{-1}]

1. Introduction

1.1. Background and problem statement

The last report issued by the World Meteorological Organization (WMO) to bring together the latest climate change updates has revealed that greenhouse gases (GHG) emissions keep increasing. The COVID-19 crisis provides only limited mitigation in global emissions. The CO_2 levels in the northern hemisphere exceeded 415 ppm in the first part of 2021, compared to 410 ppm in 2020, setting a new high record. The report also emphasizes that some climate system changes are irreversible, and many local, federal, and international strategies need to be adopted to slow or stop the other changes (World Meteorological Organization. 2021)

The demand for energy and resources is rising exponentially due to population growth (Bharathiraja et al. 2016). Between the years 2014 and 2035, an extra $40 trillion in expenditures will be required to fulfill the world's expected energy demand; 70 % of this amount will be spent on fossil fuels since fossil fuels account for the most significant proportion of transportation and heating (Vertès et al. 2020). About 330 million tons of platform chemicals are produced from fossil-based feedstocks (oil, coal, and gas). In the beginning, building blocks predominate, which are then transformed into a massive of different fine and specialty chemicals (Pachapur et al. 2016).

Over the past several decades, significant work has been done to create technology and techniques for commercial-scale biofuel production (Vertès et al. 2020). Conventional chemicals magnify worries about global warming, fossil fuel depletion, increasing environmental contamination, and increased energy inputs. Bio-based chemical synthesis has been based on using pure or simply fermentable substrates. The fermentation process is the most significant way to make renewable compounds. It requires less pressure, temperature and uses low-cost renewable resources like industrial waste, municipal trash, or treatment sludge (Pachapur et al. 2016).

The biomass feedstock is converted into biofuels (bioethanol, biomethane, biodiesel) and bio-based chemicals like LA. Numerous kinds of biomass, including lignocellulosic materials (wood and straw), starch, sugars, algae, and other organic waste products, may be used in this industrial process. It is a viable option for replacing "petroleum refineries" and reducing the reliance on fossil fuels for many industrial (S.J. Sarma et al. 2016).

LA is an important organic acid with hydroxyl and carboxylic acid groups, enabling it to engage in unique and beneficial chemical reactions (Joglekar et al. 2006). Because LA has a chiral structure, it has been widely utilized in the food, cosmetic, and Pharmaceutical industries (Phanthumchinda et al. 2018). LA is also a monomer in manufacturing biodegradable Poly Lactic Acid (PLA), which is utilized in medical applications. In addition, it looks and performs similarly to the polyethylene used in plastic films. Hence, it is one of the best plastic substitutes for those concerned about the environment (Krishna et al. 2019). The potential applications of LA are summarized by (Bisaria 2014) and illustrated in **Figure 1**

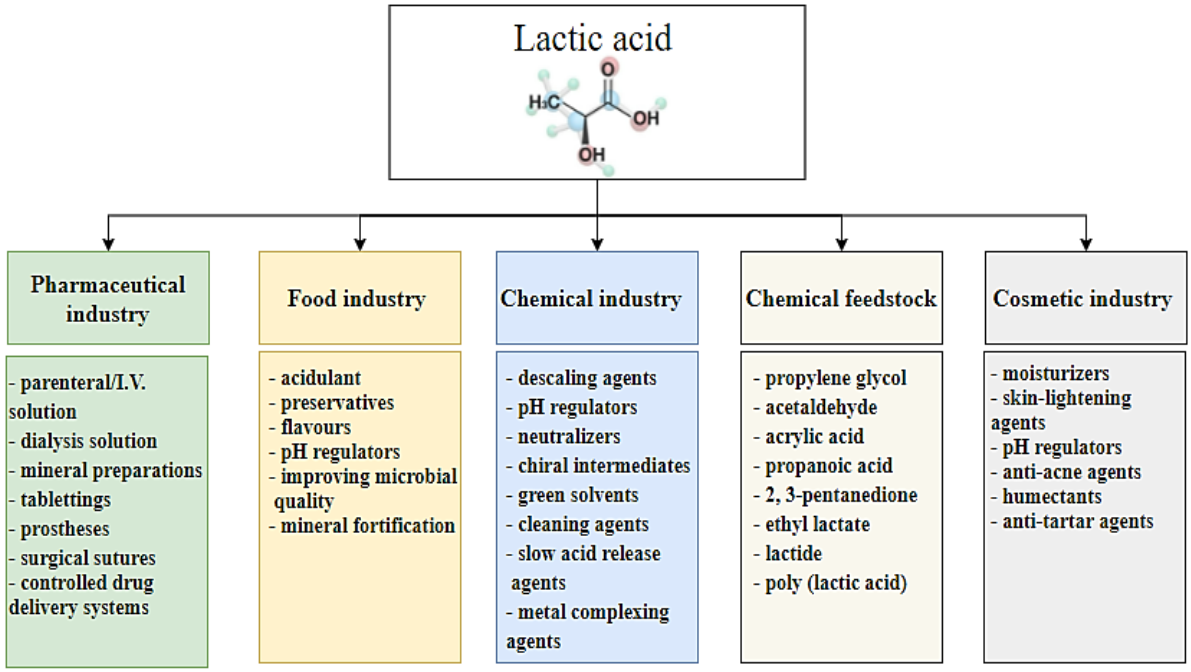

Figure 1. The potential application of lactic acid adopted from (Bisaria 2014).

According to Grand View Research, the worldwide lactic acid market in 2020 was worth USD 2.7 billion and is projected to rise at an 8.0 percent compound annual growth rate (CAGR) between 2021 and 2028. (Grand view Research. 2021)

L A may be manufactured via fermentation or chemical synthesis (Eş et al. 2018). chemical production leads to racemic mixtures of DL-lactic acid, which is unsuitable for Food, Pharmaceutical, and medical industries; therefore, about 90 percent of lactic acid is manufactured via fermentation (Alves de Oliveira et al. 2018b).

The fermentation process includes two main processes (Krishna et al. 2019), upstream and downstream processes. In upstream processing, refined starch and cellulose materials are commonly used as raw materials for LA production. In contrast, Downstream processing includes recovery and purification of LA in the fermentation broth. However, there are considerable challenges associated with the biological synthesis of LA. The primary challenges associated with the fermentation process include the cost of substrates, food competition, strains, inhibition due to substrate or product, and waste formation (Alves de Oliveira et al. 2018b). LA production by cells lowers the pH of fermentation broths, requiring base titration to maintain the proper operating PH value at 5.5-6.5. Acids are also used to control pH in upstream and downstream processes. However, adding acid and base leads to high salt levels in the fermentation broth. Also, using low-cost food waste and agricultural residues as feedstock may increase contaminants such as organic acids, proteins, and inorganic substances, making it challenging to separate microbial products.

The complex chemical nature of the fermentation broth and high concentration of contaminants such as organic acids(such as amino acids), proteins(such as glycine), residual sugar compounds, and inorganic substances complicate the downstream processing (Pleissner et al. 2017).

Several processes and technologies are utilized to recover LA, such as precipitation, distillation, solvent extraction, adsorption, and membrane separation (Electro dialysis (ED), reverse osmosis(RO), ultrafiltration(UF), nanofiltration(NF)). However, there are still many drawbacks related to the low selectivity of targeted acid, high cost, high energy consumption, and high chemical waste. Membrane-based technology has received much interest among the unit operations mentioned previously because of its environmental friendliness and ease of scaling up. Furthermore, UF and NF could be coupled with Bioreactor in one unit, enabling simultaneous production and purification, eliminating the need for additional separation units. (Komesu et al. 2017).

1.2. Previous studies of lactic acid recovery via the Nanofiltration process

Numerous research has been published about lactic acid recovery from fermentation broth. (Ecker et al. 2012) reported the purification of LA and Acetic acid (AA) from grass silage in a pilot plane using six different NF Membranes. Besides the membrane material, the variation of pH value and diafiltration approach was observed to optimize the process.

The results showed that decreasing pH plays a central role in decreasing LA rejection. Meanwhile, no effect on the transport of AA through the membranes was recognized. A pH-variation from 3.9 down to 2.5 reduced the retention of the LA significantly from 67% to 42% for the membrane DL (Osmonics). A diafiltration rate up to D = 1.5 enhanced the transport of LA into the permeate; however, more water (D > 1.5) decreased the efficiency of the separation process and increased the amount of AA lost to the permeate. Although a reasonable separation rate for the main components LA and AA from grass silage was achieved, high pure products require further treatment.

Another study (González et al. 2008) described NF. Spiral wound and tubular membrane modules to purify lactic acid from clarified fermentation broths. Flow rate, the concentration of feed, transmembrane pressure, and pH all impacted flux and rejection and the effectiveness of the NF. Membranes were linked with the combined effects of both size and charge. After analyzing the data, the electrostatic impact emerged as the major limiting factor in the lactic acid recovery using NF. LA and inorganic salts in the fermentation broth were rejected at 35–58 percent and 45–76 percent, respectively, under acidic conditions. Both pH and pressure boosted the lactic acid rejection, but increasing pH slowed the flow. The feed flow rate, which affects the concentration polarization, has little impact on the membrane's performance. The results showed that the degree of membrane surface charge affected lactate retention. Lactate rejection was higher for the DK2540C membrane at high pH levels despite the higher molecular weight cut-off (MWCO) of the AFC80 membrane.

No studies related to the influence of residual sugar on the recovery of lactic acid were found.

1.3. Aim of the work

This thesis aims to optimize the recovery of lactic acid from the grass silage model solution by investigating the effect of residual Glucose and Fructose in the model solution. For this purpose, four different NF membranes with different MWCO were tested, and two experimental approaches were followed. The first approach aimed to determine the best operation parameter with high LA concentration in permeate, through testing the membranes with a diluted solution of lactic acid (LA with deionized water), under different temperatures (25- 40 °C) and pH values (2,6- 3,8 – 6).

The second approach was to test all the membranes at chosen operation parameter with varying compositions of model solution and observe the transport behavior of LA through the membranes. The collected data from this experimental work is the basis for further modeling and simulation works that can describe this effect mathematically.

2.Grass silage

2.1. Lignocellulosic

The primary disadvantage of utilizing food materials in first-generation biorefineries is the rivalry for arable land between food production for biorefinery and for human feed, which eventually raises the commodity price of food materials (Dutta et al. 2016). Using lignocellulosic biomass (LCB) from the agro-food sector, such as lignocellulosic residues or specialized crops, instead of food resources, seems to be an excellent option for the second generation biorefinery. LCB comprises three significant polymers: cellulose, hemicellulose, and lignin, present in varying amounts and configurations depending on biomass (Bichot et al. 2018).

Some most essential chemicals from lignocellulosic biomass are summarized in Figure 2

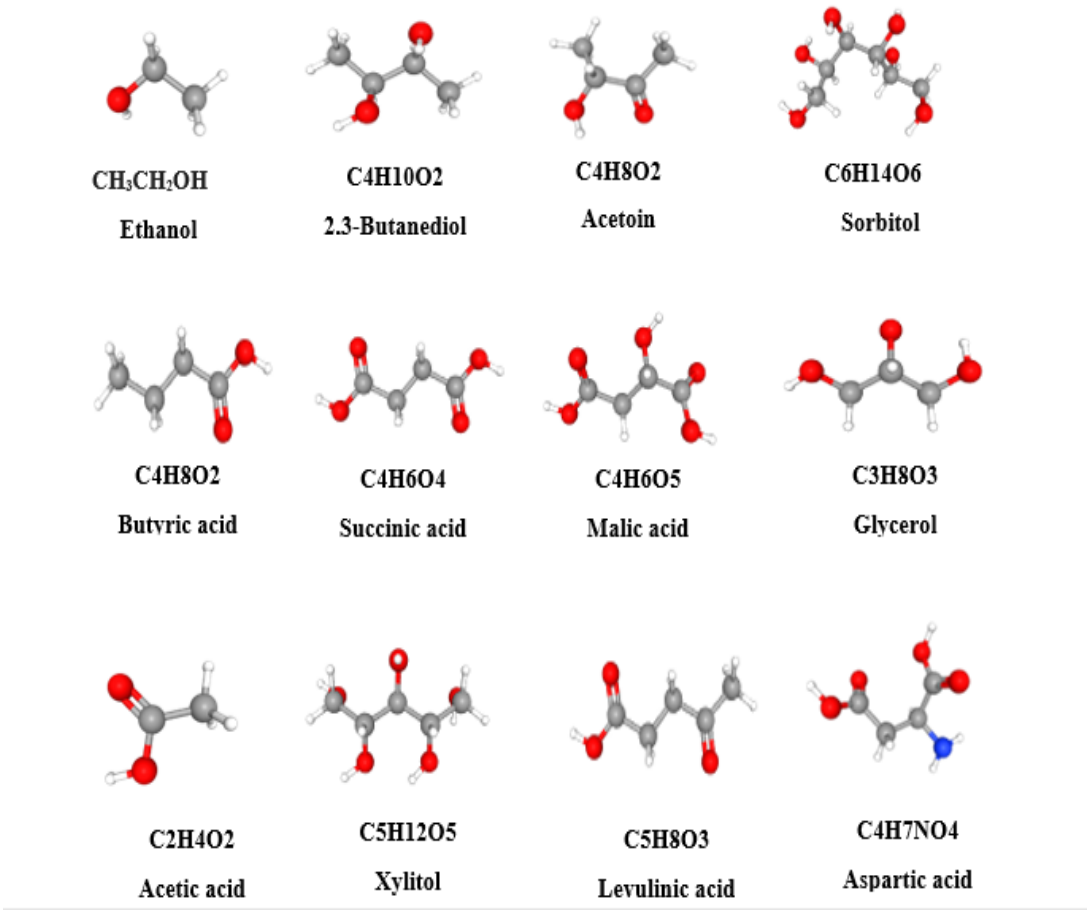

Figure 2. Some chemical platforms can be derived from lignocellulosic biomass, adopted from (S.J. Sarma et al. 2016).

LCB materials must be pretreated to utilize the unique properties of various components (cellulose, hemicelluloses, and lignin). The objective of the pretreatment is to increase access to cellulose components via enhancing the surface area, degrading lignin and hemicellulose structures, reducing cellulose crystallinity, or breaking up p-hydroxycinnamic acid linkages with other components. Cellulose degradation product is glucose, while hemicelluloses result in different molecules: C6 hexoses (glucose, mannose, or galactose) and C5 pentoses (xylose and arabinose) (Bichot et al. 2018).

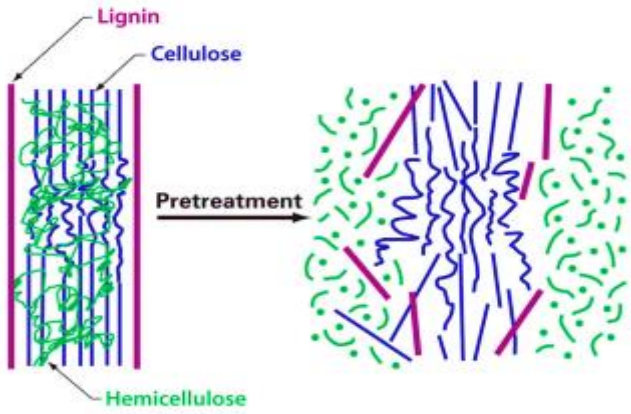

Figure 3. Deconstruction of the lignocellulose structure (Brandt et al. 2013).

Numerous pretreatment and extraction techniques have been developed to valorize lignocellulosic biomass (**Figure 4**), including physical, physicochemical, chemical, and biological processes.

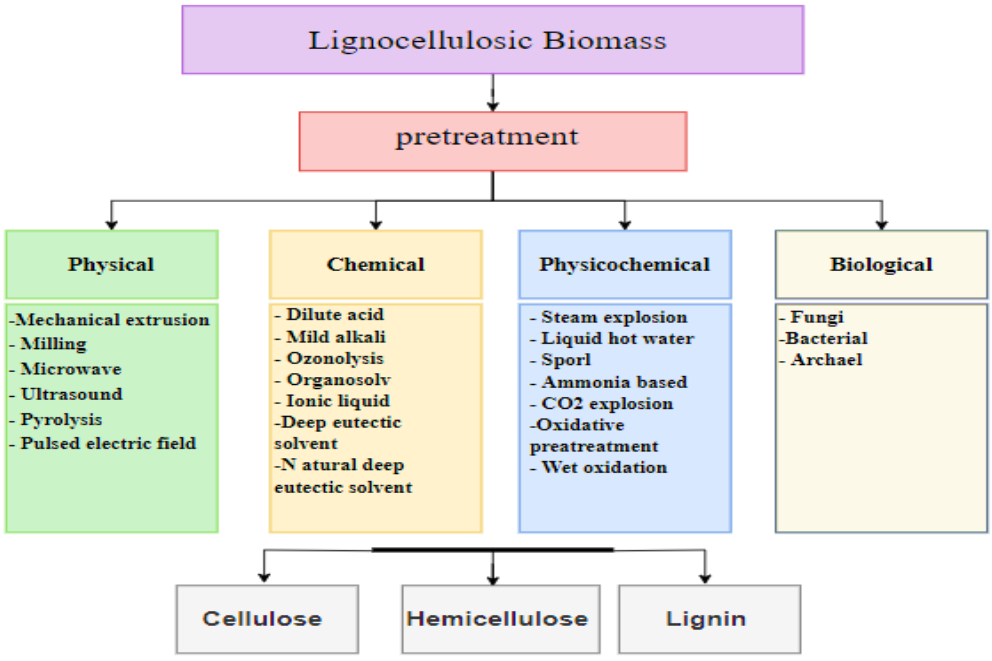

Figure 4. Pretreatment methods available for lignocellulosic biomass (Garedew et al. 2020).

2.2. Grass silage importance and production

Grassland and agriculture residues are high potential resources of LCB, especially in Europe. Besides their high availability, they can be grown and harvested on non-arable land. Experts estimate that accessible grassland biomass may reach 500,000-1,000,000 tons of dry matter in Austria alone (Kromus et al. 2004). There were 938.000 hectares of grassland in the Netherlands in 2012. Grass and other lignocellulosic biomass, like wood, provide 170 G tons of green biomass to the world each year. However, only 6 G tons are collected and utilized, mainly for food (62%) and energy production (Bichot et al. 2018).

In order to provide consistent and known quality feedstock for an anaerobic digestion plant, grassland biomass is likely to be collected and stored as silage. Ensiled grass offers more logistically efficient use of green biomass and ensures year-round availability of the raw material (Franco et al. 2019).

According to (Finch et al. 2014), silage production, also known as ensilage, is the anaerobic conversion of plant carbohydrates to lactic and other organic acids. It is critical to maintain an anaerobic environment to avoid aerobic spoilage microorganisms, which include (molds, yeasts, and aerobic bacteria) since many of these microorganisms can flourish at a low pH (4,0) but need oxygen to develop. As a result, silo sealing is essential for establishing and sustaining an anaerobic environment. During fermentation, bacteria and plant enzymes interact with the carbohydrates and proteins in the crop to produce a fermentable product. Bacteria naturally exist in the corp or could be inoculant additives to enhance the fermentation. The fermentation process leads to a fast decrease in the silage's pH to about 4; this occurs due to the formation of lactic acid and other organic acids.

Well-fermented silage is characterized by rapidly increasing lactic acid concentration and stable pH value at about 4; silage of this kind will be light brown, have a strong smell, and taste acidic. While poorly fermented silage is characterized by the formation of weaker acid called butyric acid, higher pH value of around 5, it will have green olive color and a terrible odor.

In addition to the dry matter percentage and pH, the proportion of total nitrogen in the silage as ammonia is one of the most helpful indicators of silage quality by analysis. The proportion of nitrogen should be kept to a minimum (3–5 %) to have well-fermented silage; excessive proportion (20-30 %) indicates poor fermentation and the dominance of butyric acid.

Ensilage grass is used then as raw material in a green biorefinery to produce bio-based products and energy. It starts by fractionating the biomass into liquid and solid phases. The organic juice may be utilized to make amino acids and other platform chemicals like lactic acid, while the solid waste can make fiber goods or biogas (Haag et al. 2016).

Finch et al. 2014 has also listed some factors that affect silage fermentation :

- **Type of corp**

  Three main characteristics of crops play an essential role in the ensiling process, the proportion of fermentable carbohydrates, minerals, and moisture concentration. Crops such as whole-crop corn and cereals with a high level of sugar and starch have a remarkable ability to make good silage. In contrast, crops such as alfalfa, short leafy grass, and legumes with a high level of structural carbohydrates (cellulose and hemicellulose) are viewed as challenging to ensile. Crops with high mineral concentrations (phosphates, sulfates, nitrates, and chloride) have high buffering capacity, contributing to the resistance to decrease the PH value; thus, high minerals concentration harms the ensiling process. The crop's moisture content influences the speed and extent of fermentation at ensiling. A drier crop is more favorable for ensiling, while ensiling excessively moist crops increase the opportunity for clostridia and enterobacteria to grow, resulting in high acid contents and yield losses. Apart from the fermentation effects, excessively moist crops are likely to generate effluent, and those kept overly dry are more susceptible to heating and rotting. (Muck und Kung 2007)

- **Fertilizer treatment**

  Late or excessive fertilizer treatments may result in a decrease in the proportion of sugar in the grass and the presence of high amounts of ammonia in the final silage, both of which are undesirable.

- **Weather**

  Whether that is dry and sunny is preferable for silage

- **Minimizing contamination**

  avoiding soil contamination by cutting the grass, advisable hight at 7.5–10 cm

- **Wilting**

  in order to increase dry-matter levels wilting has become a regular procedure after cutting the grass.

- **Harvesting**

  The grass is harvested through metered chop machines with a high output. Wilted grass is typically cut to between 20 and 50 mm. Finely chopped material consolidates better and allows faster achievement of full anaerobic conditions in the clamp. Additionally, fine cutting leads to a faster release of sugars from grass for fermentation. sting

- **The use of silage additives**

  many silage additives have been applied to improve the conservation and the nutritive value of grass silage. These additives Inhibit the development of aerobic microorganisms, reduce the development of anaerobic organisms which are undesired, Increase the availability of fermentable substrates for bacterial fermentation. Include helpful bacteria to ensure fermentation is dominated and adjust the ensiling conditions (Muck und Kung 2007). The most common additives are Acids and Their Salts (e.g., dilute hydrochloric and sulphuric acids), molasses, anhydrous ammonia, urea, a variety of enzymes (Pectinases, cellobiase, amylases, and glucose oxidase), and Inoculants(lactic acid-producing bacteria (LAB)).

  Nowadays, inoculants have gained widespread acceptance, primarily since they are entirely safe. It is possible to use two types of LAB: homofermentative, which produces primarily lactic acid and a rapid drop in pH, thereby preserving sugar and protein levels in the crop; and heterofermentative, which produces both lactic acid and acetic acid, resulting in a slower fermentation but inhibiting yeasts and molds.

2.3. Grass silage characteristics

The composition of grass silage changes significantly according to the art of corp and additives used in the ensiling process.

The contents of Dry matter (DM), Neutral detergent fiber (NDF), organic matter (Lactic acid, acetic acid…), crude protein (CP), and pH value are the main characteristics of grass silage.

(Franco et al. 2019) has evaluated the impact of silage characteristics on biorefinery efficiency and found a high correlation between liquid yield and dry-matter concentration.

The green juice derived from grass silage contains, besides LA and AA, various organic and inorganic components, including sugars, organic acids (acetic acid), and inorganic ions. Ca^{+2}; Mg^{+2}; K^{+}; SO_4^{-2} or macromolecular compounds (proteins) (J. Ecker et al. 2012).

The chemical and physical characteristics of grass silage juice, which is utilized as feed in an upper Austrian green biorefinery, are given in the Table

Table 2-1 The chemical and physical properties of the grass silage juice (Ecker et al. 2012)

LA, g/L	20.4
Acetic acid, g/L	3.31
AA (sum), g/L	19.3
Arginine, g/L	1.91
Aspartic acid, g/L	2.04
Leucine, g/L	1.84
Glucose, g/L	4.27
Fructose, g/L	6.53
Ca^{2+}, Mg^{2+}(sum) , g/L	1.09
Cl^{-}, g/L	1.01
SO_4^{2-}, g/L	0.23
Other salt components (Na^{+}, K^{+}, NH_4^{+}), g/L	4.2
Conductivity, mS/cm	23.1
pH, -	3.9
Density, Kg/L	1.12
Dry matter, g/L	102

3.Lactic acid

3.1. Physical and Chemical Properties

Lactic acid is a three-carbon organic acid. One of the terminal carbon atoms is a part of an acid or carboxyl group, the other terminal carbon atom is a part of methyl or a hydrocarbon group, and the central carbon atom is a part of an alcohol group. The lactic acid in its pure form is a white crystalline solid with a low melting point; carbon, hydrogen, and oxygen are present in amounts of 40 %, 6.71 %, and 53.29 %, respectively. (Auras et al. 2010). In taste, LA is non-volatile, odorless, and mildly acidic; it is soluble in water and water-miscible organic solvents but not in organic solvents. LA has two optical isomers L(+)-lactic acid and D(–)-lactic acid. (Kumar et al. 2019)

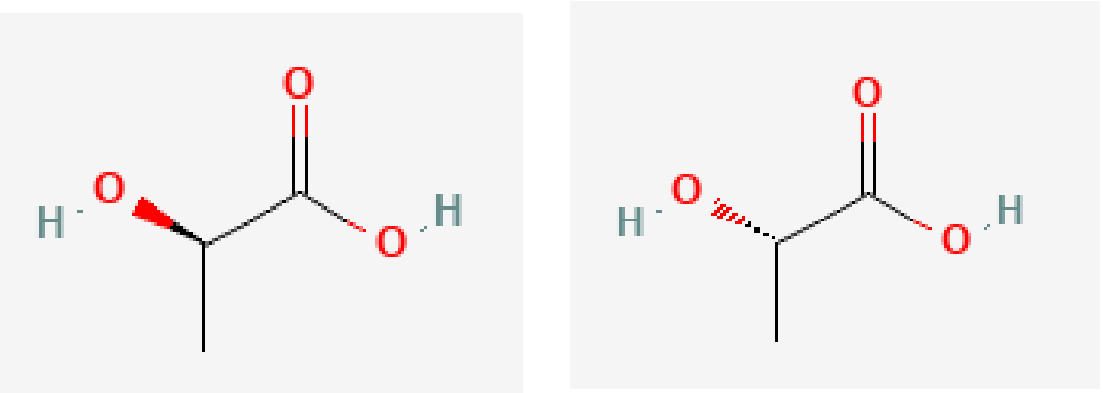

Figure 5. LA isomers , D(-)-lactic acid (left) , L(+)-lactic acid (right).

Some physical and chemical properties of lactic acid are shown in **Table 3-1**

Table 3-1 Physical and chemical properties of lactic acid (Kumar et al. 2019)

Properties	Value
Chemical formula	C3H6O3 or CH3CHOHCOOH
Functional groups	Carbonyl group C=O and the hydroxyl group –OH
IUPAC name	2-hydroxy propanoic acid or 2- hydroxy propionic acid
Other names	Milk acid or Three carbon acid or Alpha hydroxy acid (AHA)
Assay	88–92%
Odour	Odourless
Molecular weight (MW)	90.08 g/mol
Isometric purity	Minimum 95% L (+)
Dissociation constant (pKa)	3.86
Colour	Colourless (at 15 °C and 1 atm)
Normal boiling point, °C	122 at 14 mmHg
Melting temperature, °C	L: 53 D: 53 D/L: 16.3
Heat of combustion, ΔHc	1361 kJ/mol
Specific heat, Cp at 20 °C	190 J/mol/°C
Appearance	Yellow to colourless crystals (syrupy 50% liquid)
Specific gravity (20/20)	1.02–1.22
Flashpoint, °C	110
Solubility	Soluble in water, furfural, slightly soluble in ether, and insoluble in carbon disulfides and petroleum ether

3.2. Lactic acid production

Lactic acid can be synthesized chemically or biologically. Chemical synthesis produces lactic acid as a racemic mixture of the isomers L- and D-lactic acid. This method is primarily based on the hydrolysis of lactate with strong acids. Other chemical methods to lactic acid synthesis are possible but are neither technically nor commercially viable. Meanwhile, biotechnological procedures have several benefits, including utilizing renewable natural biomasses as substrates. Furthermore, biotechnological methods synthesize optically pure L-lactic acid or D-lactic acid, depending on the strain used. (Rodrigues et al. 2017)

3.2.1. Biotechnological process

Renewable resources (wheat, maize, whey, molasses, starch, cellulose) are utilized as raw materials. These resources are pretreated using the saccharification technique (hydrolysis) to get fermentable carbohydrates from polysaccharides. This is followed by free cell fermentation, which can be a batch-wise or continuous operation. Calcium hydroxide is added to the fermentable carbohydrate in a neutralization step, resulting in calcium lactate formation. The crude calcium lactate is purified and hydrolyzed through concentrated H_2SO_4 or HCl. Then, in the esterification stage, methanol is added to LA to produce methyl lactate, which is then purified via distillation and hydrolyzed once more with water to yield LA and methanol (Kumar et al. 2019).

the main reactions involved in classical lactic acid fermentation and recovery are listed below (Yang et al. 2013)

1- Neutralization

$$C_6H_{12}O_6 + CA(OH)_2 \longrightarrow (2CH3CHOHCOO^-)Ca^{+2} + 2H_2O \quad (1)$$

2- Hydrolysis by H_2SO_4

$$(CH_3CHOHCOO^-)Ca^{+2} + H_2SO_4 \longrightarrow 2CH_3CHOHCOOH + CaSO_4 \quad (2)$$

3- Esterification

$$2CH_3CHOHCOOH + CH_3OH \longrightarrow 2CH_3CHOHCOOH_3 + H_2O \quad (3)$$

4- Hydrolysis by H_2O

$$2CH_3CHOHCOOH_3 + H_2O \Longrightarrow 2CH_3CHOHCOOH + CH_3OH \quad (4)$$

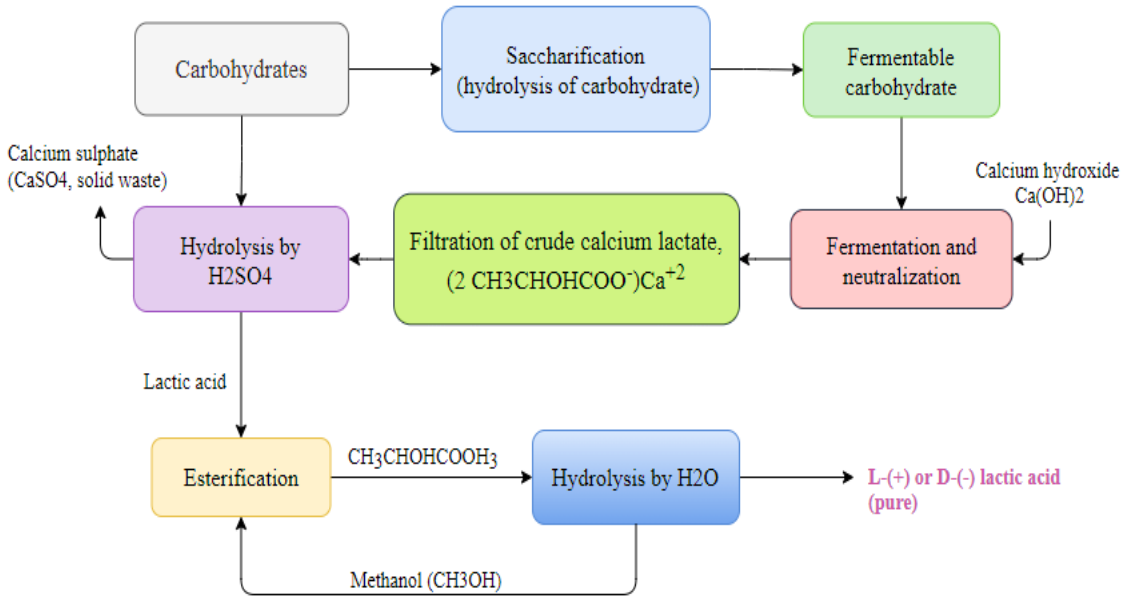

Figure 6. The conventional method for producing lactic acid, adopted from (Kumar et al. 2019).

The classical fermentation process still faces many challenging aspects regarding used raw materials, pH control, and downstream processing. While refined materials such as glucose, sucrose, and lactose may significantly decrease product purification costs and eliminate the saccharification step, which requires enzymes or acids, it is not cost-effective due to the high production costs (Krishna et al. 2019). Meanwhile, the usage of hydrolysates also includes difficulties regarding the hydrolyzing conditions, the high cost of enzymatic hydrolysis, which is more effective than acidic hydrolysis, and the complex composition of the resulted fermentation broth, which cause complexity in the subsequent separation and purification processes (Rodrigues et al. 2017). Utilizing CaCO3 or Ca(OH)2 to neutralize and regulate the pH during batch fermentation creates a significant issue in solid waste treatment since a considerable quantity of $CaSO_4$ is generated and accumulates in the environment.

Numerous methods have been suggested to address these issues. In bacterial fermentation, alternating alkalis such as NH_4 OH, liquid NH_3, and NaOH have replaced the traditional lime

method. Continuous operation instead of batch fermentation can reduce lactic acid accumulation and increase productivity. However, high lactic acid concentrations were not obtained, a series of membrane cell recycle bioreactors was utilized to enhance LA concentration (Yang et al. 2013).

Many research has been conducted to improve the productivity and viability of bioprocesses on a broad scale using alternative methods. Such as the Co-culture method in which two or more cell populations with varying degrees of interaction are grown together to generate a particular product. Also, Continuous Stirred Tank Reactors (CSTR) have been extensively utilized because of their high capacity and controlled production parameters (Eş et al. 2018).

3.2.1.1. Microorganisms

Various microorganisms may generate lactic acid, including bacteria, fungus, yeast, and cyanobacteria. The strain selection process is critical, particularly in reducing nutritional needs, secreting high optical purity lactic acid, and encouraging high yields and productivities.

- **Bacteria**

  Traditional LA manufacturing has relied on LAB, and it remains the most likely option for industrial (Bisaria 2014).

  LAB is generally divided into four main categories: Lactic Acid Bacteria (LAB), Escherichia coli, Corynebacterium glutamicum, and Bacillus strains, and into two types based on the fermentation patterns: homofermentative or heterofermentative Bacteria.

  Homofermentative: Bacteria in this category use the Embden–Meyerhof–Parnas (EMP) glycolytic pathway to convert glucose to lactic acid. They do not ferment pentoses and gluconates. They ferment 1 mol glucose to 2 mol lactic acid and provide a net output of 2 mol ATP for every mole of glucose metabolized. Lactic acid is the primary product of this fermentation

  Heterofermentative: Bacteria in this group generate 50 % lactic acid, 50 % ethanol (or acetic acid), and 50 % CO_2 from glucose. They use the phosphoketolase-dependent route to convert 1 mole of glucose to 1 mol of lactic acid, 1 mol of ethanol (or acetic acid), and 1 mol of CO_2. One mol of ATP is produced for every mol of glucose. The metabolic pathway of the bacteria in both types are shown in **Figure 7**
  (Yang et al. 2013).

  LAB has certain drawbacks, including the synthesis of L- and D-lactic acid, a poor yield owing to by-product generation, and a high risk of bacteriophage infection lysis (Rodrigues et al. 2017).

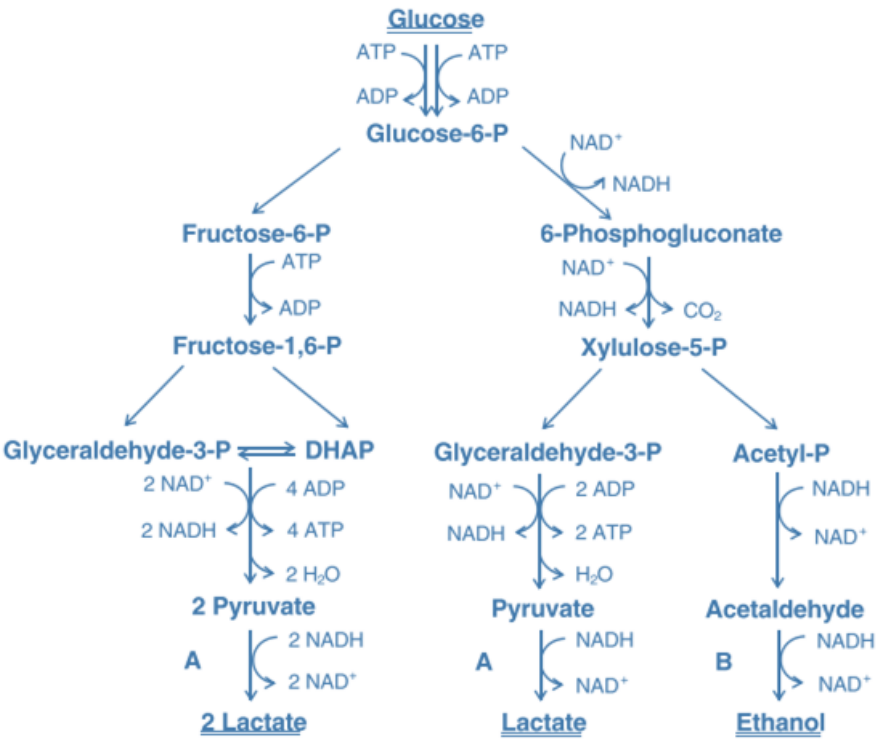

(a) Homofermentative metabolism (b) Heterofermentative metabolism

Figure 7. Metabolic pathways of lactic acid bacteria (Yang et al. 2013).

- **Fungi**

Fungi such as Rhizopus can create only optically pure l-lactic acid. It also secretes hydrolytic enzymes capable of digesting raw materials such as starch-rich agricultural residues and pentose sugars in plant biomass. As a result, Rhizopus eliminates the requirement for hydrolysis, which is often needed in bacterial fermentation, and reduces inhibition caused by glucose buildup, resulting in increased productivity, decreased reactor volume, and lower capital expenditures (Yang et al. 2013).

The primary disadvantage of lactic acid generation by fungus is that the lactic yield is lowered since carbon produces by-products other than lactic acid. The limits of lactic acid generation by fungus include mass transfer restrictions, which result in a limited production rate, and the need for intense aeration since it is an aerobic process (Krishna et al. 2019).

- **Yeasts**

Lactic acid production is inefficient when wild-type yeast is used as a feed source., However, with the development of genetic engineering, yeasts genetically designed to produce a large yield of lactic acid have been developed. The primary benefits of employing yeast as a nutrition supply are their tolerance for low pH (1.5), limiting the regeneration of precipitated calcium lactate, hence lowering the cost of neutralization using neutralizing agents such as calcium carbonate. The most significant disadvantage of employing yeast as a nutrition source is that it increases manufacturing expenses (Krishna et al. 2019).

3.2.2. Downstream process

Downstream processing is a final and critical process for biotechnology-based product creation since the concentrations of the target products are often slight. This reality indicates lengthy, challenging, and energy-intensive procedures that may threaten the fundamental foundations of biotechnology. According to some writers, downstream processing costs may account for up to 50% of the total costs for specific product manufacturers. Many separation technologies have been proposed and adapted for the recovery of LA. in the following, the essential purification methods of LA from fermentation broth will be reviewed

3.2.2.1. Neutralization and Precipitation

Neutralization and precipitation is the classical process for recovering lactic acid and are discussed in 3.2.1. many studies have reported the effect of replacing Calcium hydroxide with other neutralization agents such as NH_4OH, NaOH, and $Mg(OH)_2$ to improve the purity of LA. Magnesium lactate was discovered to have a much higher purity than calcium lactate and ammonium lactate. The formed magnesium lactate reacts with trimethylamine to give a complex (trimethylamine-LA, or R_3N-LA); this complex is further thermally decomposed to give LA a purity of 99 % (Meng et al. 2020).

- **advantages**: Easy operation (Ahmad et al. 2020)
  Accessible in process intensification (Ahmad et al. 2020)
  High yield (Alves de Oliveira et al. 2020)

- **disadvantages:** Many filtration steps (Alves de Oliveira et al. 2020)
  Environmental problems (Alves de Oliveira et al. 2020)
  A large amount of waste generation (Alves de Oliveira et al. 2020)
  Massive wastewater generation (Ahmad et al. 2020)
  Poor product purity (Ahmad et al. 2020)

3.2.2.2. Ion exchange / Adsorption

In general, the separation of lactic acid using ion-exchange includes three stages, lactate ion adsorption, elution, and lactate conversion into lactic acid, and requires several ion-exchange operation processes. In the typical operating procedure (**Figure 8**), fermentation broths pass filtration and enter a cation exchanger column, where acidification occurs. Sodium lactate is converted to lactic acid through an exchange of sodium ions for hydrogen ions. When the pH of the effluent rises, the resin becomes saturated with the sodium ion, and all undissociated lactic acid passes through the column. Then undissociated lactic acid is absorbed in anion exchange column and separated from fermentation broth. At this step, elution by liquid adsorption occurs, and lactic acid is recovered through the eluent (Din et al. 2021).

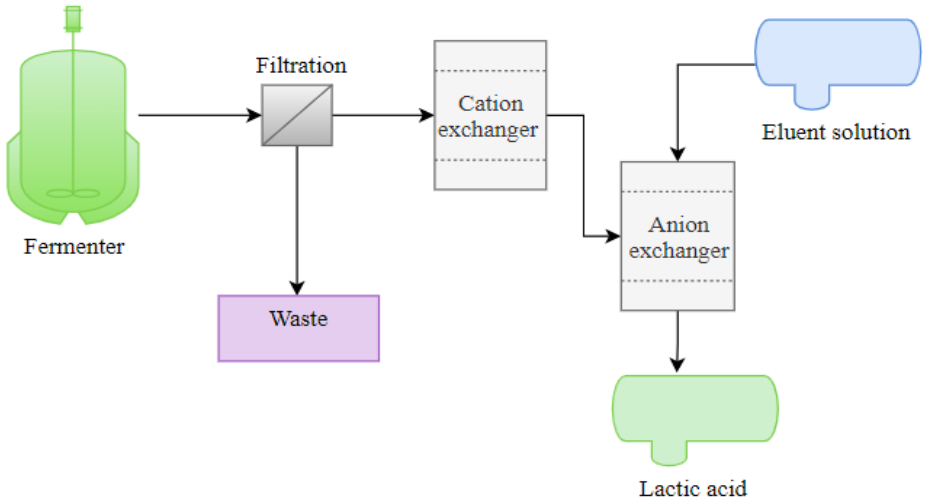

Figure 8. Schematic diagram of the extractive ion-exchange lactic acid process adopted from (Din et al. 2021).

- **Advantages:** High selectivity
  Low energy consumption
  Reduction of chemical utilization (Alves de Oliveira et al. 2020)
- **Disadvantage:** High cost
  Generation of waste streams for resin regenerating
  PH dependent (Alves de Oliveira et al. 2020)

3.2.2.3. Reactive extraction

Reactive extraction is a kind of solvent extraction in which the LA acid (target molecule) forms a complex with an extractant that has a higher affinity for an organic solvent (diluent) than for the aqueous phase (fermentation broth). Extractant and LA acid create a compound through ion pairing and hydrogen bonding. A further stage of back extraction is needed to recover the free acid and renew the extractant. (Alves de Oliveira et al. 2020), The most effective extractant used for LA extraction are Alamine 336 in methyl isobutyl ketone, Alamine 336 in decanol, and a mixture of tripropylamine and trioctylamine in 1-octanol / n-heptane (Beschkov und Yankov 2021)

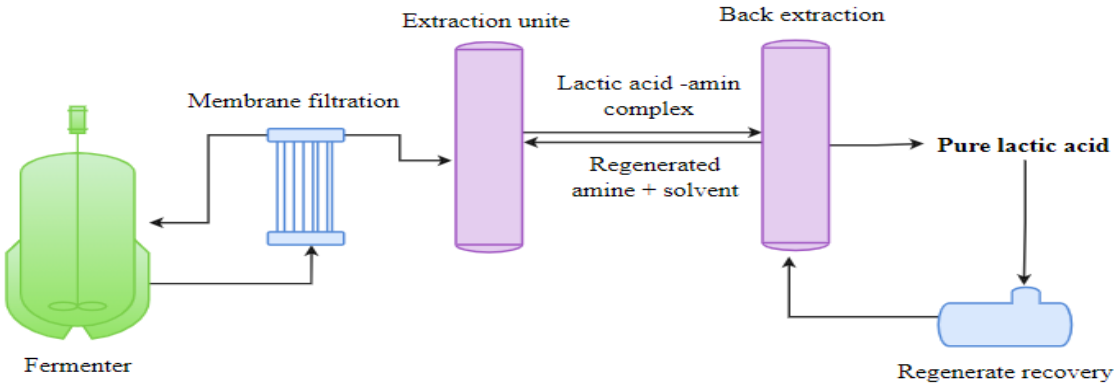

Figure 9. Reactive extraction of lactic acid (Alves de Oliveira et al. 2020).

- **Advantages:** Simple and high selectivity (Ahmad et al. 2020)
  Economical and clean process (Ahmad et al. 2020)
  End-product inhibition (Alves de Oliveira et al. 2020)
- **Disadvantages:** No high purity of the product
  Need the stripping method to regain the solvents
  Organic solvent toxicity toward microorganism

3.2.2.4. Reactive distillation and Molecular Distillation

Reactive distillation is an alternative to the traditional process, it involves chemical reaction (Esterification) and distillation process in one unite. In the Esterification step, the LA in fermentation broth reacts with lower alcohols (Methanol and Ethanol) to form esters, which have a lower boiling point than LA. The relevant esters are obtained and subsequently hydrolyzed to generate a mixture of LA and alcohol. LA is obtained at the bottom of the distillation tower, while alcohol can be recovered at the top (Meng et al. 2020).

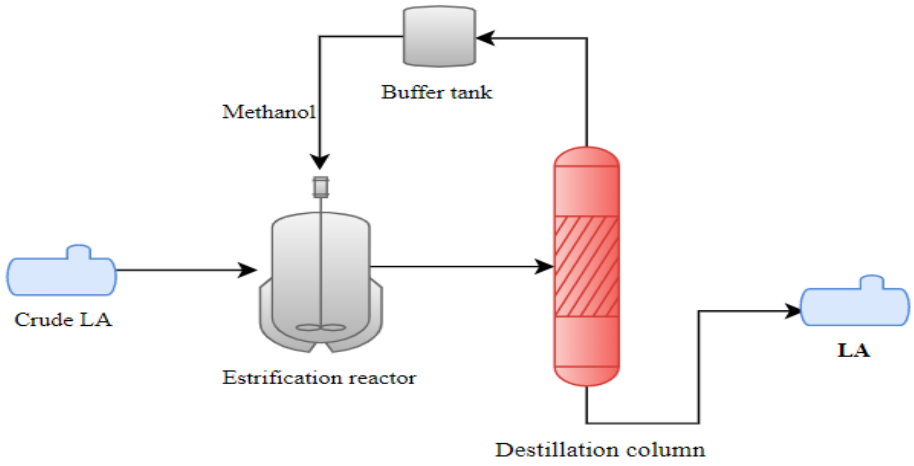

Figure 10. Reactive distillation processes for LA purification (Meng et al. 2020).

- **Advantages:** A high degree of purification
  Fewer energy requirements
  Single unit process for reaction and separation (Ahmad et al. 2020)

- **Disadvantages:** Complicated process
  Still Energy-intensive process (Ahmad et al. 2020)
  separation of the azeotropes of ester-alcohol (Meng et al. 2020)

Molecular distillation is A novel liquid-liquid separation approach based on molecular mean free path difference; it is carried out under a high vacuum and lower temperature. The process occurs in the evaporation chamber under a vacuum; the light molecule evaporates on the heating surface and then returns to the liquid phase on the condensation surface. At the same time, the residue flows down the sidewall at the evaporator; the distance between evaporator and condenser is less than the average molecular free path, which ensures high purity of light molecule. (Li et al. 2021)

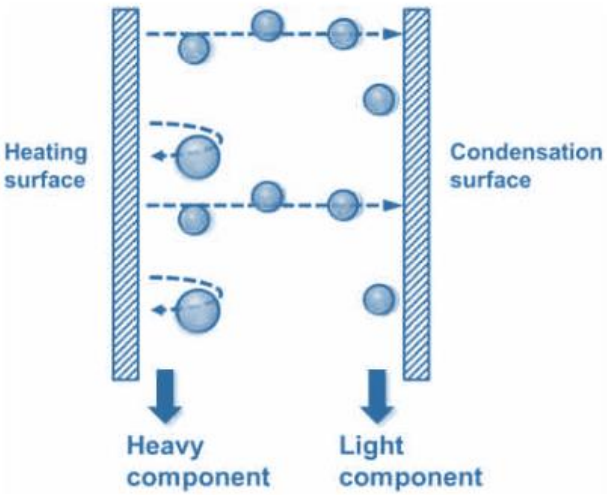

Figure 3. 1. Schematic for molecular distillation (Meng et al. 2020).

- **Advantages:** Fewerseparation steps
  Reduces risk of thermal decomposition
  High purity (Alves de Oliveira et al. 2020)
- **Disadvantages:** High vacuum conditions
  Difficulties for scaling up (Alves de Oliveira et al. 2020)

3.2.2.5. Electrodialysis

Electrodialysis (ED) is utilized extensively with ultra and nanofiltration to recover organic acids. Membranes are positioned in an alternating manner between the cathode and the anode. A direct external current (electric field) transports the cation to the cathode and the anion to the anode to accomplish separation. Two types of electrodialysis have shown high efficacy in lactic acid separation: monopolar and bipolar electrodialysis membrane. First, lactate is concentrated employing desalting in monopolar ED; then, in bipolar (ED), water is electrolyzed into H^+ and OH^- to turn lactate into high-purity LA and recover alkali for the adjustment fermentation process pH (Li et al. 2021).

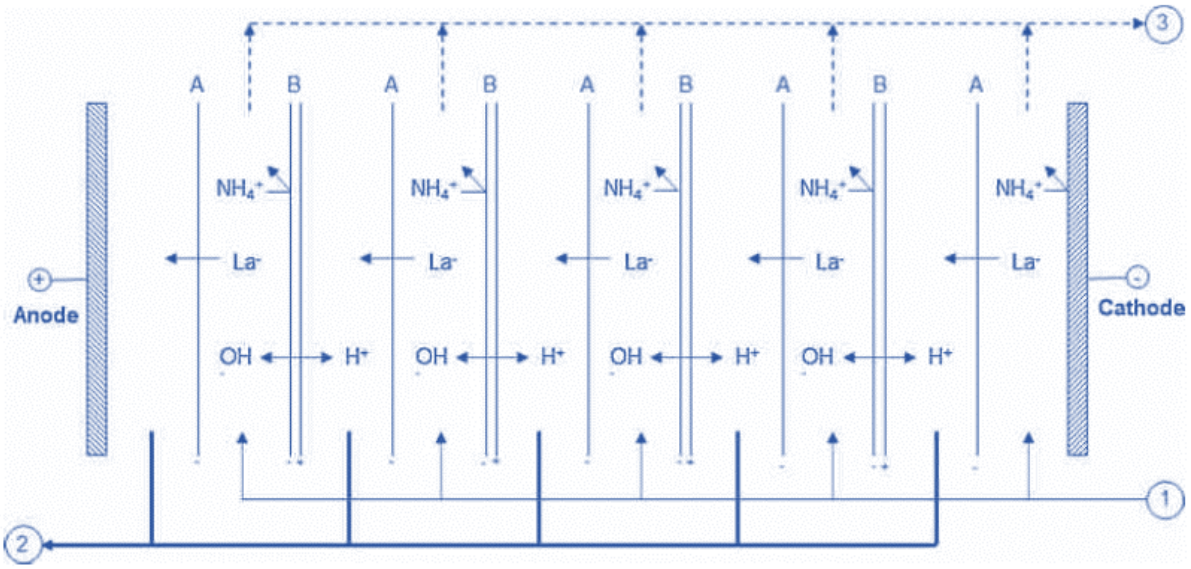

Figure 11. Schematic diagram of bipolar membrane electrodialysis for lactic acid separation: (1) LA fermentation broth, (2) Concentrated LA product, (3) Recovery of ammonia, A- Anion exchange membrane, B- Bipolar membrane, LA: lactic acid. (Li et al. 2021)

- **Advantages:** Environmental-friendly (Alves de Oliveira et al. 2020)
  The high degree of separation (Ahmad et al. 2020)
  The possibility of chemical recycling (Alves de Oliveira et al. 2020)

- **Disadvantage:** Fouling of the membrane
  High operational cost
  Pretreatment required (Ahmad et al. 2020)

In addition to ED, other Membrane processes have been utilized to achieve high purity of LA, such as micro and ultrafiltration as pretreatment stage to remove most contaminants. At the same time, nanofiltration can efficiently retain most sugars, pigments, and divalent salt ions. Since the nanofiltration was analyzed within the scope of this work, it will be discussed in more detail in the following chapter.

Table 3-2 Most recent downstream studies for lactic acid recovery

Separation method	LA Feedstock	LA final concentration g /L	Yield (%)	LA final purity (Wt %)	Reference
Molecular distillation	Fermentation broth	-	74,09	95,6	(Alves de Oliveira et al. 2018a)
Solvent extraction + Molecular Distillation	Fermentation broth	-	74	92.39	(Li et al. 2021)
Amberlite resins IRA-67	Processed Eucalyptus wood	21	99	-	(Din et al. 2021)
Amberlite resins IRA-67 and IRA-400	Cheese whey	143,7	13,40	100	(Din et al. 2021)
IRA-67 and IR-120	Date pulp waste	-	91	94.6	(Ahmad et al. 2021)
Three-stage membrane-integrated hybrid reactor system	Fermentation broth	250	96	95	(Alves de Oliveira et al. 2018a)
Reactive distillation	Synthetic	347,68	99,94	-	(Alves de Oliveira et al. 2018a)
	Fermentation broth	-	89.7	90	(Li et al. 2021)
Simulated moving bed (SMB) chromatography (PVP) resins.	Fermentation broth	-	> 93	99.9	(Yang et al. 2013)
Precipitation	Fermentation broth	-	89.7	71.49	(Ahmad et al. 2020)
Cross-flow nanofiltration	Fermentation broth	-	-	85,6	(Alves de Oliveira et al. 2018b)

4.Basics of membrane technology

The term "membrane" refers to a selective barrier that separates two homogenous phases. Continuous steady-state membrane processes consist of three streams: feed, product (permeate), and reject (retentate). The dashed line in the process boundary represents the semipermeable barrier that enables some components to pass but not others (Singh 2015).

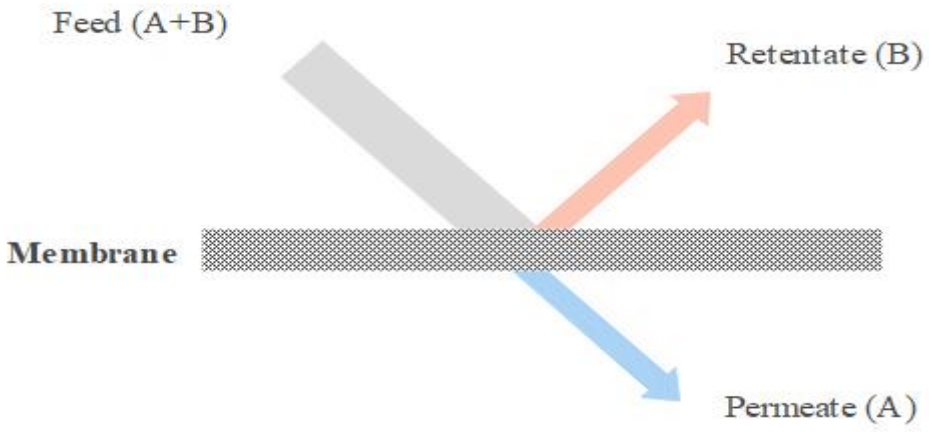

Figure 12. The basic principle of membrane processes adopted from (Cui et al. 2010)

4.1. Membrane classification

Membranes are classed according to various factors, including their type, structure, and separation mechanism. Biological membranes are classified as living or nonliving, whereas synthetic membranes are classified as organic (polymeric or liquid) or inorganic (ceramic or metal). Membranes are classified into two types based on their structure or morphology: symmetric (isotropic) and asymmetric (anisotropic) (Purkait und Singh 2018).

- **Isotropic membranes:** are uniform in chemical composition and physical characteristics throughout the entire membrane. The symmetric membranes can be either porous, in which the separation is primarily determined by the size of the molecules and the distribution of pore sizes (Micro/Ultrafiltration). Or it can be a dense film in which the transport occurs by diffusion under the driving force of pressure,

concentration, or electrical potential gradient. Or it can be an Electrically charged membrane such as electrodialysis. The separation, in this case, is based on the diffusivity and selectivity of the ions across the membrane (Baker 2012).

- **Anisotropic membranes:** are made up of two layers that differ in polymer chain arrangement and, in some instances, chemical composition across the membrane cross-section (Xiao 2017)

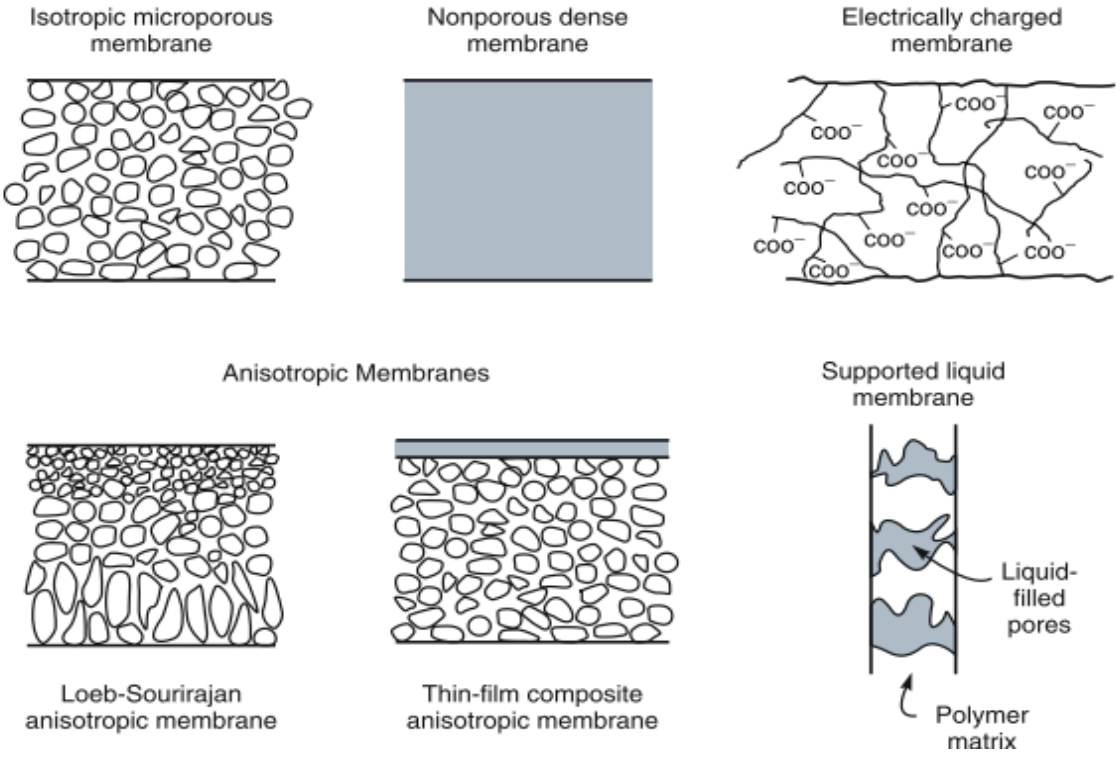

Figure 13. Schematic diagrams of the isotropic and anisotropic Membranes (Baker. 2012)

Xiao. 2017 has classified the membrane based on its manufacturing material into :

- **polymeric membranes:** Polymers are still the most widely utilized materials for membrane manufacturing, accounting for over 90 % of commercial membranes. Polysulfone (PSF), polyethersulfone (PES), cellulose acetate (CA), polyimide (PI), polyvinyl alcohol (PVA), polyvinyl fluoride (PVDF), and polydimethylsiloxane are all available for membrane production
- **Metallic membranes:** Stainless steel, nickel (Ni), titanium (Ti), and their alloys have been primarily employed to make porous membranes. However, their industrial applications on a large scale are restricted owing to their expensive cost.

- **Ceramic membranes**: such as alumina (Al2O3), zirconia (ZrO2), carbides, borides, nitrides, and silicides
- **composite materials**: such as polymer and inorganic filler, also called mixed matrix material (MMM)
- **Liquid membrane** involves a liquid that is immiscible with the source(feed) and receiving (product) solutions that serve as a semipermeable barrier between these two liquid and gas phases

according to the nature of the driving force, the membrane process can be classified into three types (Purkait und Singh 2018)

- **Pressure-Driven Processes:** MF, UF, NF, and RO
- **Concentration-Driven Processes:** Gas separation(GS), Pervaporation (PV), and Dialysis
- **Electrically Driven Processes:** Electrodialysis

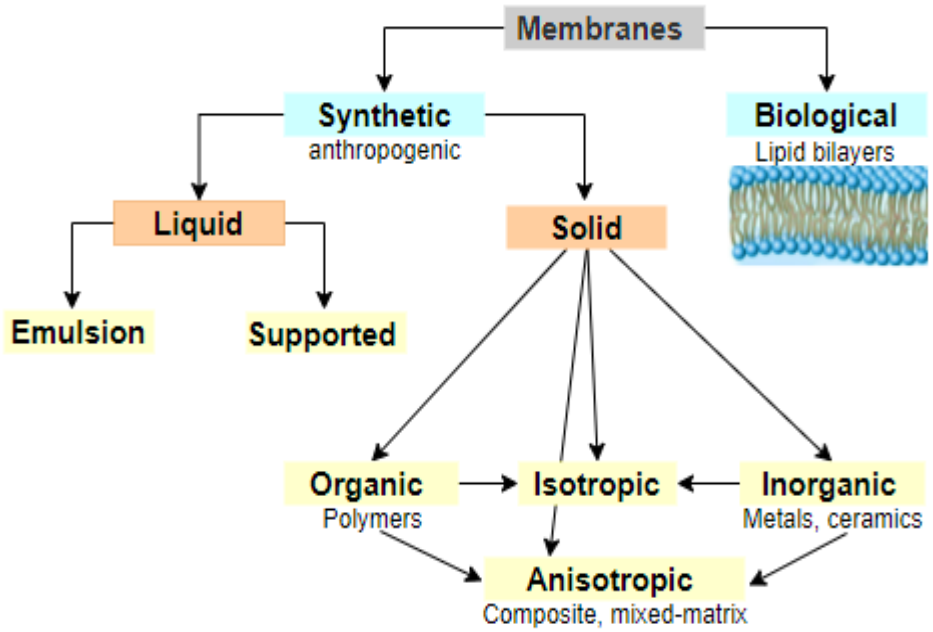

Figure 14. General classification of membranes according to origin and materials (Melin und Rautenbach. 2007)

4.1.1. Pressure- Driven membrane process

Pressure-driven membrane processes are extensively employed in various sectors, including chemistry, pharmaceuticals, biotechnology, desalination, food, and dairy. Pressure is used to drive feed separation into permeate and retentate in this membrane process. These membranes are often composed of polymers, ceramics, metals, or organometallic compounds. This process is classified based on membrane pore size; therefore, separation happens in these processes based on the size exclusion mechanism. The different membrane processes under this category are microfiltration, ultrafiltration, nanofiltration, and reverse osmosis (Purkait und Singh 2018)

- **Microfiltration:** in the MF membrane, the pore size varies from 100 nm to 10000 nm, and the pressure needed for the separation is low and ranges from 10 kPa to 300 kPa. MF can separate suspended particles, silt, algae, protozoa, and bacteria.
- **Ultrafiltration:** the pore size varies from 1 to 100 nm, and the operating pressure ranges from 200 to 1000 kPa; UF can effectively separate colloids, suspended solids, and organic molecules of higher molecular weight. A pore-flow model can best describe transport in UF and MF membranes. (Purkait und Singh 2018)
- **Nanofiltration:** The pore size of NF membranes is generally between 0.5 and 2 nm, which corresponds to a molecular weight cut-off (MWCO) of 300–500 Da. The separation performance of NF membranes is dictated by the sieving (steric hindrance) and /or Donnan (electrostatic) effects. (Xiao 2017)
- **Reverse osmosis:** RO membranes are typically dense membranes with pores less than 1 nm in diameter. Generally, they are a skin layer inside the polymer matrix. Membrane material (polymer) is layered and web-like in structure. The solution–diffusion process governs the transport of penetrants across the membrane. (Purkait und Singh 2018)

Pressure-driven membrane processes have two operating modes: dead-end and cross-flow

- **Dead-end**: one feed stream enters the membrane module and runs vertically to the membrane surface.
- **Cross-flow:** one feed stream tangentially approaches the membrane surface, and two streams exit the membrane module, one for retentate and one for permeate.

The tangential flow in cross-flow mode assists shear away rejected species at the membrane surface, restricting cake layer heights and sustaining the permeate flux. (Cui et al. 2010)

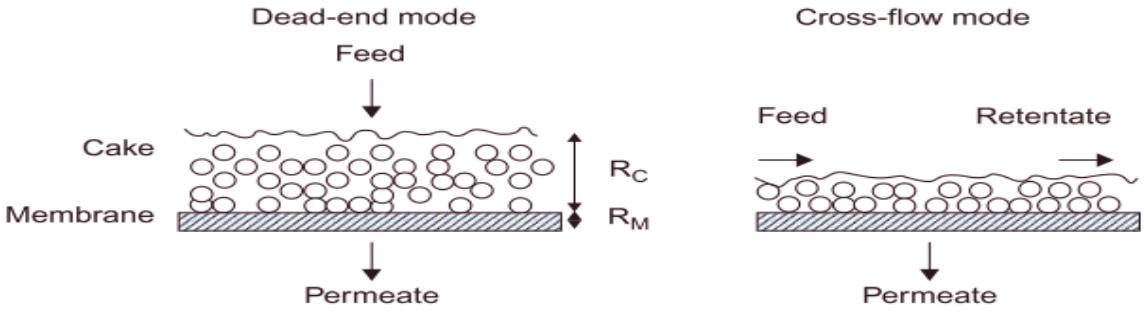

Figure 15. The schematic diagrams of the dead-end and cross-flow modes(Cui et al. 2010)

Table 4-1 Characteristics of Pressure-driven Membranes (Tewari 2015).

Process	Membrane type and pore size	Membrane material	Operating Pressure	Applications
MF	Symmetric microporous, 0.1–10 µm	Cellulose nitrate or acetate, PVDF, PTFE, metal oxides	10–500 kPa	Separation of suspended solids, bacteria
UF	Asymmetric microporous, 2–100 nm	Polysulfone, polypropylene, Nylon 6, PTFE, PVC, acrylic copolymer	0.1–0.5 Mpa	Separation of macromolecules and virus
NF	Asymmetric skin-type, 0.5–2.0 nm	Cellulosic acetate, aromatic Polyamide	0.5–2 Mpa	Separation of bivalent ions and macromolecules
RO	Asymmetric skin-type, 0.3–0.5 nm	Cellulosic acetate, aromatic Polyamide	2–10 Mpa	Separation of monovalent salts and microsolutes

4.2. Membrane modules

Membrane modules include flat-sheet, tubular, capillary, and hollow-fiber membranes. Flat-sheet membranes are manufactured in plate-and-frame, rotating disk, spiral-wound, annular-gap dynamic membrane modules, and pleated membrane cartridge designs. Tubular membrane modules include tubular, capillary, and hollow-fiber membranes. As a result, membrane modules are selected following the numerous treatment targets.

- **Plate–Frame Module**

  The flow channel is between the flat membrane plates, and the permeate is received from the interior of the flat membrane plate. Flat membrane modules are of two types: plate–frame and stack. The plate–frame has a low membrane layer density but can be used for a feed with high suspended material concentration by adjusting the spacing between spacers. In contrast, the stack configuration can achieve a high membrane layer density by horizontally piling up membranes.

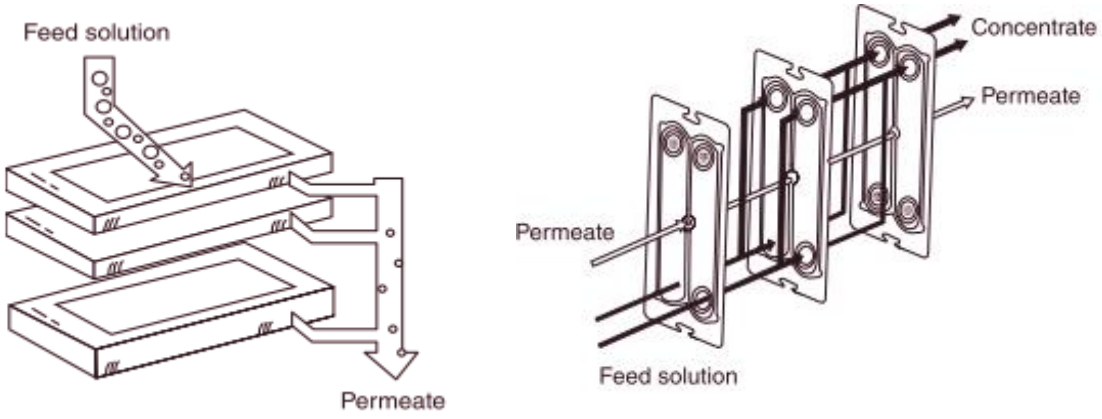

Figure 16. Plate frame model ,stack type (link), Plate-frame-type (right) (Uragami 2017)

- **Spiral Module**

  A permeable flat-sheet membrane is spirally wound around a central core, comparable to a cloth roll. The permeable membrane is sealed at its borders and gapped with a spacer material that enables the filtered liquid to pass through. Liquid enters one end and is filtered within the module using back pressure to force the clean liquid through the membrane surface. (permeate) can be gathered at the module's opposite end. Poor

cleaning options are disadvantageous. On the other hand, good material exchange through feed spacers is advantageous.

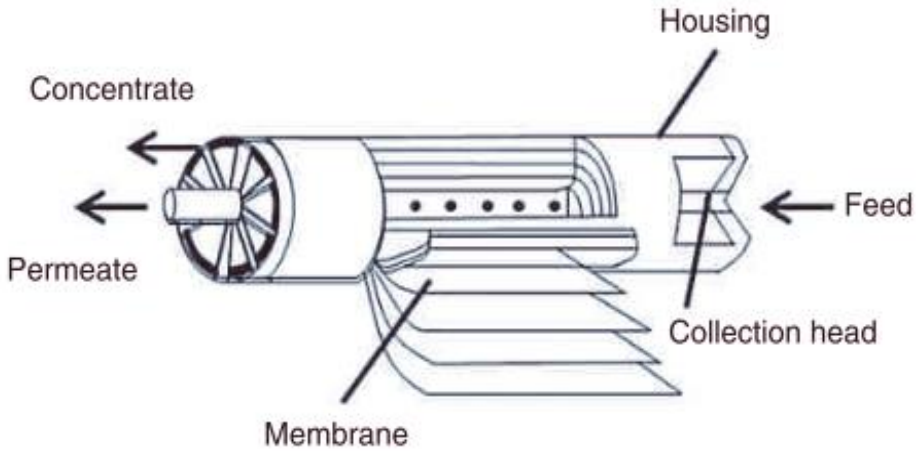

Figure 17. Spiral module (Uragami 2017)

- **Tubular Module:**

  Tube modules are often constructed using porous ceramic or stainless-steel tubular membranes. The tube's interior diameter is more than 3–5 mm. Membranes with sizes smaller than this are capillary or hollow-fiber membranes. The skin layer is cast on a ceramic or stainless-steel support. Disadvantages are low packing density (<200 m^2 / m^3) and a large feed volume flow per membrane area. On the other hand, the possibility of cleaning and low-pressure loss are advantages.

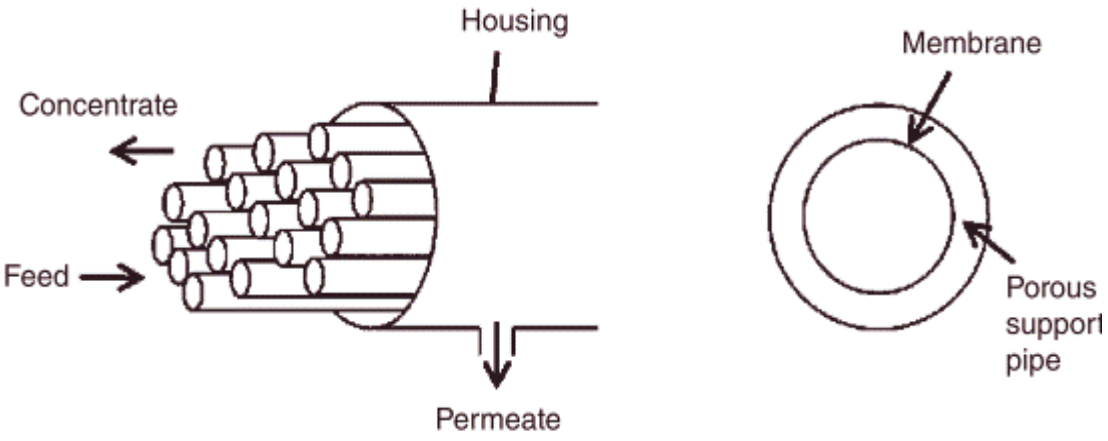

Figure 18. Tubular module (Uragami 2017)

- **Hollow-Fiber Module**

  This module is housed in a tubular housing with the membrane element enclosed on one or both sides by a bundle of hollow fibers with an internal diameter smaller than 1 mm. Because the hollow fiber serves both as a separator and support, no material for the flow is needed. As a result, the membrane's density and volume efficiency can be increased. There are two kinds of operation strategies for hollow-fiber modules: pressurized and immersion. Additionally, the former kind is classified as internal and external pressurized. The feed is filtered from inside to outside the membrane in the internal type, unlike the external type. Predominantly laminar flow is disadvantageous if there is internal flow (poor mass transfer). On the other hand, a higher packing density than a tube module is advantageous (Uragami 2017).

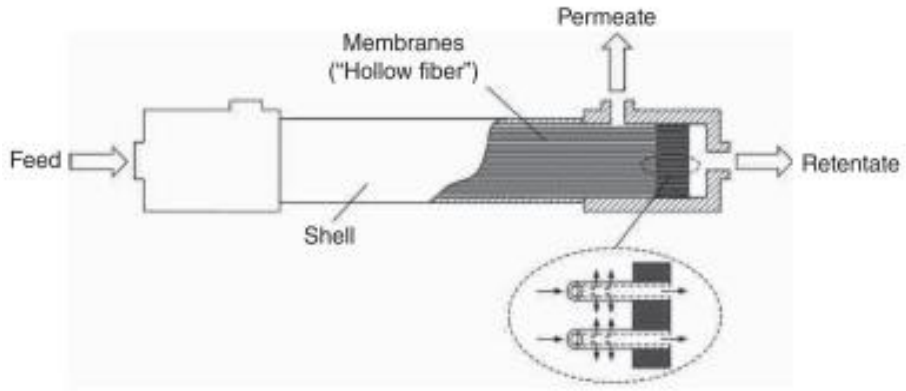

Figure 19. Hollow-fiber membrane (Chong und Fane. 2021)

4.3. Membrane transport

Transport mechanisms of solute/solvent molecules through membranes are generally divided into four types

1- Bulk flow through pores

2- Diffusion through pores

3- Restricted diffusion through pores

4- Solution-diffusion through dense membranes

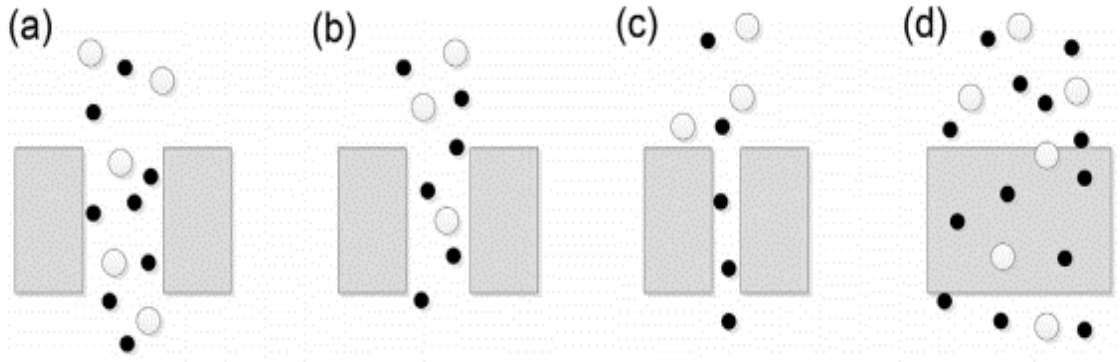

Figure 20. Transport mechanisms in membranes. (Flow is downward.) (a) Bulk flow through pores; (b) Diffusion through pores; (c) Restricted diffusion through pores; (d) Solution-diffusion through a dense membrane (Ang und Mohammad 2015).

The efficiency and productivity of membrane separation procedures can be evaluated using two fundamental parameters: Flux and Selectivity. The productivity is characterized by the permeate flux (J), which reveals the rate of the mass flow through a membrane area

$$J = \frac{M}{A\,t} = \left[\frac{Kg}{m^2 s}\right] , \left[\frac{L}{m^2 s}\right] \qquad (4.1)$$

M is the total mass transferred over time t through a membrane area A

$$J = k \times X \qquad (4.2)$$

X is the potential gradient per unit membrane thickness, where k is the proportionality factor. In the case of concentration-driving force, Fick's law describes the relationship between the flow of a material and a concentration gradient; the proportionality constant is the diffusion coefficient. Ohm's law describes the relationship between an electrical current and an electrical potential gradient, while Fourier's law describes the relationship between

heat transfer and a temperature gradient. Proportionality, in a general sense, refers to a membrane's resistance to the transport of a penentrant. (Xiao 2017)

Fick's law: $J = D.\ \Delta C$ (4.3)

Ohm's law: $I = \Delta U/R$ (4.4)

Fourier's law: $Q = k\Delta.\ T$ (4.5)

Hagen–Poiseuille's law $V = h_d.\ \Delta p$ (4.6)

the efficiency of the membrane process is characterized by selectivity (S); selectivity is defined as the ability of a membrane to differentiate between the components of a mixture, allowing some to permeate through and rejecting the others

$$S_{ij} = \frac{y_i / y_j}{x_i / x_j} \quad (4.7)$$

where y, x are the mole fraction in permeate and feed, respectively.

Besides selectivity, the Rejection coefficient, R, is a reliable indicator of the separating ability of a membrane process

$$R = 1 - \frac{C_{P,i}}{C_{R,i}} \quad (4.8)$$

4.3.1. Concentration polarization

In pressure-driven liquid-phase processes, solutes and particles transfer to the membrane surface with the solvent by convection; The accumulation of retained species close to the membrane is known as concentration polarization, represented by the concentration gradient adjacent to the membrane as depicted in Figure 4.9. The balance between convection toward the membrane (J) and back-transport from the membrane to the bulk (C) determines the amount of concentration polarization. Mechanisms that induce back-transport of solutes include:

- molecular (Brownian) diffusion
- shear-induced diffusion
- interaction-induced migration (due to electro-kinetic and surface forces)

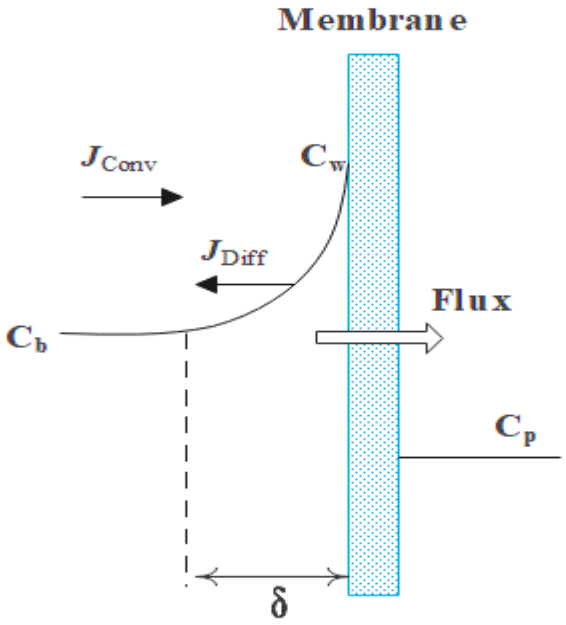

Figure 21. Solute concentration gradient, Adopted from (Chong und Fane 2021).

Diffusive back-transport is the most common back-transport mechanism represented by the mass transfer coefficient, k (=D/δ). The well-known film model is obtained by a boundary-layer mass balance where net convection = back-diffusion,

$$J \cdot C - J \cdot C_p = - D \cdot dC/dy \qquad (4.9)$$

which, after integration over the boundary layer (y =0 to δ and $C = C_W$ to C_b), gives for a fully retained species ($C_p = 0$),

$$J = k \ln (C_W / C_b) \qquad (4.10)$$

$$J = k \ln (C_W - C_P / C_b - C_P) \qquad (C_p > 0) \qquad (4.11)$$

C_b, C_W, and C_p are the solute concentrations in bulk , at the membrane surface, and at the permeate side. Eq (4.10) shows that flux is directly related to the mass transfer coefficient. The surface concentration CW is exponentially related to the flux to mass transfer coefficient ratio (J/k) for a given flux. Conversely, the ratio, C_W/C_b, known as the polarization modulus M, is given by,

$$M = C_W / C_b = \exp (J / k) \qquad (4.12)$$

M Increases with increasing J (higher flow of solutes to the membrane surface means increasing C_w) and decreasing k (=D/δ). The magnitude of M depends on the solute diffusivity. Thus, for typical fluxes and low molecular compounds such as inorganic ions (salts), M is < 2,0 for large organic macromolecules such as humic acids; M is >5,0, and in the case of proteins, M can be >10.

The increasing of CP module can increase solute transmission, osmotic pressure difference (OPD), and fouling; it also reduces the separation capabilities of the membrane; the observed retention is defined as,

$$R_a = (1 - C_p / C_b) \qquad (4.13)$$

however, the membrane separates depending on its intrinsic retention (R_i) and the concentration on its surface C_w, not C_b.

$$R_i = (1 - C_p / C_W) \qquad (4.14)$$

from Equations (4.11) and (4.14) :

$$R_a = \frac{Ri}{Ri+(1-Ri)\ exp\ (J / k)} \qquad (4.15)$$

As a result, the observed retention is lower than the intrinsic retention, and as the concentration polarization increases (as J/k increases), the observed retention becomes lower, and solute transmission increases; additionally, if flux is maintained, the fouling will occur, and it will

create an "unstirred" layer adjacent to the membrane, known as cake-enhanced concentration polarization (CECP) which causes the effective *k* value to decrease (Chong und Fane 2021).

4.3.2. Fouling

Due to the CP, some species deposit irreversibly on the membrane surface (not removed by zero flux operation), known as fouling. The flux is expressed in the osmotic pressure model, which relates to driving force and resistance.

$$J = \frac{TMP - \Delta\pi i}{\eta(Rm + Rf)} \tag{4.16}$$

$$\Delta\pi_i = \pi_w - \pi p \tag{4.17}$$

The fouling can also reduce the effective driving force because of CECP; The CECP leads to hindered back-diffusion of retained solute, giving higher C_W values and higher πw. Generally, fouling can be avoided by regulating concentration polarization through the flux to mass transfer coefficient ratio (*J/k*) by restricting flux and/or providing good fluid management. Module design and operation are critical in defining the value of (*J/k*) and achieving desirable values, Hence controlling C_P and mitigating the fouling (Chong und Fane 2021).

4.3.3. Transport regimes in Nanofiltration

NF membranes show a behavior between dense and microporous membranes; in addition, size exclusion and electrostatic interaction are the two fundamental phenomena that govern the solute rejection by NF (Ang und Mohammad 2015). Some of the commonly used transport models, especially for uncharged solutes (glucose, fructose, and lactic acid), will be discussed in the following section

- **Spiegler Kedem modell**

  Spiegler Kedem model is an irreversible thermodynamic model, and it involves three essential parameters: hydraulic permeability, solute permeability, and reflection coefficient. The derivation of Spiegler and Kedem model expressed the volume and the solute flux across the membrane as

$$J_V = L_P(\Delta p - \sigma\Delta\pi) \tag{4.18}$$

$$j_s = -P_s\frac{dc_s}{dx} + (1-\sigma)c_s J_V \tag{4.19}$$

  The reflection coefficient represents the separation capability of the membrane. Integrating Eq. (4.19) yields an expression of solute rejection:

$$R = \frac{\sigma(1-F)}{(1-\sigma F)} = 1 - \frac{C_P}{C_f} \tag{4.20}$$

$$\text{where, } F = \exp\left(1 - J_V(1-\sigma)/P_s\right) \tag{4.21}$$

  R is the actual rejection value that considers the concentration polarization factor, while C_P and C_f are solute concentrations in permeate and feed, respectively. The water permeability is evaluated by using Eq. (4.18), assuming the osmotic pressure difference is zero. The logarithm average concentration C_{if} is used to determine r and Ps. (Agboola et al. 2015)

- **models based on Nernst Planck equation**

  The most famous mathematical model for NF is the extended Nernst-Planck equation, and it has been employed extensively for simulating NF membranes. In order to model ion transport across the membrane, the Nernst–Planck equation incorporates the contributions from diffusion, convection, and electrical migration.

  The extended Nernst-Planck equation is given by:

$$j_{\mathrm{i}} = -c_{\mathrm{i}} D_{\mathrm{i,p}} \left(\frac{\mathrm{d}}{\mathrm{d}x}\mu_{\mathrm{i}}\right) + K_{\mathrm{i,c}} c_{\mathrm{i}} J_{\mathrm{v}} \tag{4.22}$$

The electrochemical potential μ_{i} can be expressed as:

$$\mu_{\mathrm{i}} = R_{\mathrm{g}} T \ln\ a_{\mathrm{i}} + V_{\mathrm{si}} P + z_{\mathrm{i}} F \psi + \mathrm{constan}\ t \tag{4.23}$$

Substituting Eqs. (4.23) into (17) yields:

$$j_{\mathrm{i}} = c_{\mathrm{i}} D_{\mathrm{i,p}} \frac{\mathrm{d}}{\mathrm{d}x} \ln\ a_{\mathrm{i}} - \frac{z_{\mathrm{i}} c_{\mathrm{i}} D_{\mathrm{i,p}}}{RT} F \frac{\mathrm{d}\psi}{\mathrm{d}x} - \frac{c_{\mathrm{i}} D_{\mathrm{i,p}}}{RT} V_{\mathrm{si}} \frac{\mathrm{d}P}{\mathrm{d}x} + K_{\mathrm{i,c}} c_{\mathrm{i}} J_{\mathrm{v}} \tag{4.24}$$

for low-pressure cases, the pressure effect is neglected. With $\frac{\mathrm{d}P}{\mathrm{d}x} = 0$, and the activity coefficient a_{i} for the solute in the capillary is expressed as $a_{\mathrm{i}} = c\gamma_{\mathrm{ii}}$. By substituting $\mathrm{d}\ln\ a_i = \frac{\mathrm{d}a_{\mathrm{i}}}{a}$ into Eq (4.24) gives

$$j_{\mathrm{i}} = -\frac{D_{\mathrm{i,p}}}{\gamma_{\mathrm{i}}} \frac{\mathrm{d}(c_{\mathrm{i}}\gamma_{\mathrm{i}})}{\mathrm{d}x} - \frac{z_{\mathrm{i}} c_{\mathrm{i}} D_{\mathrm{i,p}}}{RT} F \frac{\mathrm{d}\psi}{\mathrm{d}x} + K_{\mathrm{i,c}} c_{\mathrm{i}} J_{\mathrm{V}} \tag{4.25}$$

By simplifying the integration of $\frac{\mathrm{d}(c_{\mathrm{i}}\gamma_{\mathrm{i}}\mathrm{i})}{\mathrm{d}_x}$, to $c_{\mathrm{i}} \left(\frac{\mathrm{d}\ln\ \gamma_{\mathrm{i}}}{\gamma_{\mathrm{i}}}\right)$ and neglecting it, the reduced equation of the Nernst-Planck equation will be :

$$j_{\mathrm{i}} = \underbrace{-D_{\mathrm{i,p}} \frac{\mathrm{d}c_i}{\mathrm{d}x}}_{\text{diffusion}} \underbrace{- \frac{z_{\mathrm{i}} c_{\mathrm{i}} D_{\mathrm{i,p}}}{RT} F \frac{\mathrm{d}\psi}{\mathrm{d}x}}_{\text{Donnan potential}} + \underbrace{K_{\mathrm{i,c}} c_{\mathrm{i}} J_{\mathrm{v}}}_{\text{convection}} \tag{4.26}$$

The first term in Eq(4.26) represents the solute transport due to diffusion. The second term describes the solute flux due to the Donnan potential. The last term represents the solute flux contribution due to convection solute.

Many other models have been developed based on this equation, such as the Donnan-Steric-Pore model (DSPM).

In DSPM, electrostatic and steric effects characterize the solute separation behavior across the membrane. and the ionic partition coefficient of ion i is written as follow

$k_{\mathrm{i}} =$ [Steric exclusion] × [Electrostatic exclusion (Donnan)]

$$k_{\mathrm{i}} = \varphi \exp\ \left(-\frac{F z_{\mathrm{i}}}{RT} \Delta\psi_{\mathrm{D}}\right) \tag{4.27}$$

The DSPM is further developed to include dielectric effect (DE), the partition coefficient of the DSPM-ED model can be written as follow (Agboola et al. 2015)

$$k_{\mathrm{i}} = \varphi \exp\left(-\frac{Fz_{\mathrm{i}}}{RT}\Delta\psi_{\mathrm{D}}\right)\exp\left(-\frac{\Delta W_{\mathrm{i}}}{Kb\,T}\right) \tag{4.28}$$

- **Model for uncharged solutes based on Nernst Planck equation**

For uncharged solutes, only the diffusive and convective flows affect the transport of solutes inside the membrane. Thus, the molar flux of solute can be expressed as :

$$j_{\mathrm{i}} = K_{\mathrm{ic}} c_{\mathrm{i}} u + \left(\frac{-c_{\mathrm{i}} D_{\mathrm{ip}}}{RT}\frac{\mathrm{d}\mu_i}{\mathrm{d}x}\right) \tag{4.28}$$

where u is the solvent velocity and K_{ic} is a hindrance factor, and it is given thus

$$K_{\mathrm{ic}} = (2-\varphi_{\mathrm{i}})(1.0 + 0.054\lambda_{\mathrm{i}} - 0.988\lambda_{\mathrm{i}}^2 + 0.441\lambda_{\mathrm{i}}^3) \tag{4.29}$$

where φ_{i} is the dimensionless steric partition coefficient of solute i and may be expressed thus:

$$\varphi_{\mathrm{i}} = (1-\lambda_{\mathrm{i}})^2 \tag{4.30}$$

λ_{i} is the dimensionless ratio of solute radius $i(r_{\mathrm{i}})$ to the effective pore radius (r_{p}) and it is given as follows:

$$\lambda_{\mathrm{i}} = \frac{r_{\mathrm{i}}}{r_{\mathrm{p}}} \tag{4.31}$$

And D_{ip} is the pore diffusion coefficient of solute i and may be expressed thus

$$D_{\mathrm{ip}} = K_{\mathrm{id}} D_{\mathrm{i}\infty}\frac{\eta_0}{\eta} \tag{4.32}$$

where K_{id} is the ionic hindrance factor for diffusion, K_{id} maybe written as:

$$K_{\mathrm{id}} = 1.0 - 2.30\lambda_{\mathrm{i}} + 1.154\lambda_{\mathrm{i}}^2 + 0..224\lambda_{\mathrm{i}}^3 \tag{4.33}$$

the change in viscosity inside pores must be taken into account as it affects the pore diffusion coefficient, D_{ip} , The viscosity ratio is given by:

$$\frac{\eta}{\eta_0} = 1.0 + 18\left(\frac{\mathrm{d}}{r_{\mathrm{p}}}\right) - 9\left(\frac{\mathrm{d}}{r_{\mathrm{p}}}\right)^2 \tag{4.34}$$

Uncharged solute chemical potential, μ_{i} , is defined as

$$\mu_{\mathrm{i}} = R_{\mathrm{g}} T \ln\, a_{\mathrm{i}} + V_{\mathrm{si}} P \tag{4.35}$$

substituting it in Eq. (4.28) yields:

$$j_i = K_{\mathrm{i,c}} c_{\mathrm{i}}(x) u - D_{\mathrm{ip}} c_{\mathrm{i}}(x)\, \partial_{\mathrm{x}} \ln \gamma_{\mathrm{i}} - D_{\mathrm{ip}}\, \partial_{\mathrm{x}} c_{\mathrm{i}}(x) \; - \frac{1}{RT} V_i D_{ip} c_i(x) \partial_x P \qquad (4.36)$$

Because the concentration within the pore is so low, the activity coefficient term in Eq. (4.36) is neglected; the pressure gradient in the pores can be calculated by rearranging the Hagen–Poiseuille type relationship the assumption that the pressure gradient is constant along the pore.

$$\partial_x P = \frac{\Delta P_e}{\Delta x} = \frac{8\eta u}{r_p^2} \qquad (4.37)$$

where ΔP_e is the effective pressure, and it is given as

$$\Delta P_{\mathrm{e}} = \Delta P - \Delta \pi \qquad (4.38)$$

substituting it in Eq (4.36)

$$j_{\mathrm{i}} = \left[K_{\mathrm{ic}} - \left(\frac{8\eta}{RT r_{\mathrm{p}}^2} \right) D_{\mathrm{ip}} V_{\mathrm{i}} \right] c_{\mathrm{i}} u - D_{\mathrm{ip}} \frac{\mathrm{d}c_i}{\mathrm{d}x} \qquad (4.39)$$

The molar flux j_{i} is also linked by the filtration condition:

$$j_{\mathrm{i}} = C_{\mathrm{ip}} u \qquad (4.40)$$

Substituting Eqs. (4.40) into (4.39), yields

$$\frac{\mathrm{d}c_{\mathrm{i}}}{\mathrm{d}x} = \left[\left[K_{\mathrm{ic}} - \left(\frac{8\eta}{RT r_{\mathrm{p}}^2} \right) D_{\mathrm{ip}} V_{\mathrm{i}} \right] c_{\mathrm{i}} - C_{\mathrm{ip}} \frac{u}{D_{\mathrm{ip}}} \right] \qquad (4.41)$$

integration the Eq.(4.41 (with the boundary conditions) can give the relationship for the uncharged solute rejection as follow

$$R_{\mathrm{i}} = 1 - \frac{(K_{\mathrm{ic}} - \beta_{\mathrm{i}})\varphi_{\mathrm{i}}}{1 - [1 - (K_{\mathrm{ic}} - \beta_{\mathrm{i}})] \exp(P_{\mathrm{ei}})} \qquad (4.42)$$

where β_{i} and P_{ei} are the dimensionless quantity and dimensionless modified Peclet number. Where $\beta_{\mathrm{i}} = \frac{8\eta}{RT r_{\mathrm{p}}^2} D_{\mathrm{ip}} V_{\mathrm{i}}$, $P_{\mathrm{ei}} = \frac{(K_{\mathrm{ic}} - \beta_{\mathrm{i}}) r_{\mathrm{p}}^2 \Delta P_{\mathrm{c}}}{8\eta D_{\mathrm{ip}}}$. (Agboola et al. 2015)

- **Solute Partitioning Model.**

  The partition coefficient describes the relation between the solute concentration outside and within the membrane pores. ϕ can be written as

$$\phi = 2\int_0^{1-\lambda} g(\rho)\rho \mathrm{d}\rho \tag{4.43}$$

  where ρ is the dimensionless position in the pore $(\rho = r/r_p)$ (with r the radial position in the pore) and $g(\rho)$ the radial distribution function

  ϕ will be defined by equilibrium thermodynamics and will therefore be reliant on the affinity of the solute to the membrane. the radial concentration profile of the solute in the membrane pore is assumed to be governed by Boltzmann equation

$$g(\rho) = \exp\left(-\frac{\Delta G_i(\rho)}{K_b\, T}\right) \tag{4.44}$$

  $\Delta G_i(\rho)$is the free-energy difference associated with the differences in solute interactions in the water and membrane surface. After substitution of Eq (4.44) and integration, eq (4.43) then becomes

$$\phi = (1-\lambda)^2 \exp\left(-\frac{\Delta G_i}{kT}\right) \tag{4.45}$$

  according to this Eq, the partitioning of a solute is dependent on the size exclusion effects (expressed by the factor $(1-\lambda)^2$) and on solute-membrane affinity (expressed by (ΔG_i)

  (ΔG_i) can be considered to quantify attractive or repulsive solute-membrane affinity interactions, a negative value of(ΔG_i) Indicates a high affinity between membrane and solute. This will result in a lower rejection than was expected, based solely on size exclusion. However, if ΔG_i is positive (e.g., for a hydrophilic solute), there will be resistance against the partitioning of the solute into the membrane phase, resulting in a higher rejection than expected based on size exclusion

  (Verliefde et al. 2009) has reported that Partitioning Model is more reliable than traditional size-exclusion models in predicting the transport of hydrophobic solutes and membranes due to high affinity between them, while traditional size-exclusion models can well predict the transport of hydrophilic solutes

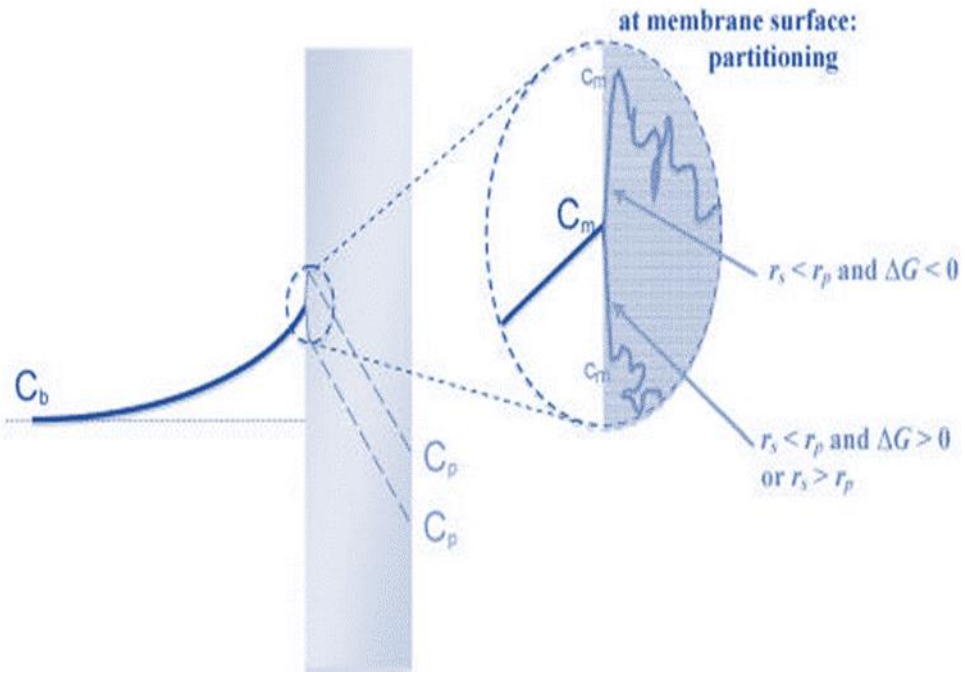

Figure 22. Conceptual mechanistic illustration of the solute-membrane size and affinity-based interactions (Verliefde et al. 2009)

5.Methodology

5.1. Experimental setup

A lab-scale cross-flow filtration membrane unit (OS-MC-01) from Osmota was used for the experiments; the unit is shown in Figure 5.1. The experimental set used works on a batch mode. A jacketed feed tank with a capacity of 2 Liters delivers the solution to a piston pump (CAT - 231), which pushes the solution through a rectangular membrane module with a 0,008 m^2 area. The retentate gets recycled into the feed tank. At the same time, the permeate was collected in becker and weighted with a digital balance. The equipment can be operated at a temperature ranging from 5 to 70 °C and a pressure up to 64 bar.

Figure 23. Membrane filtration unit.

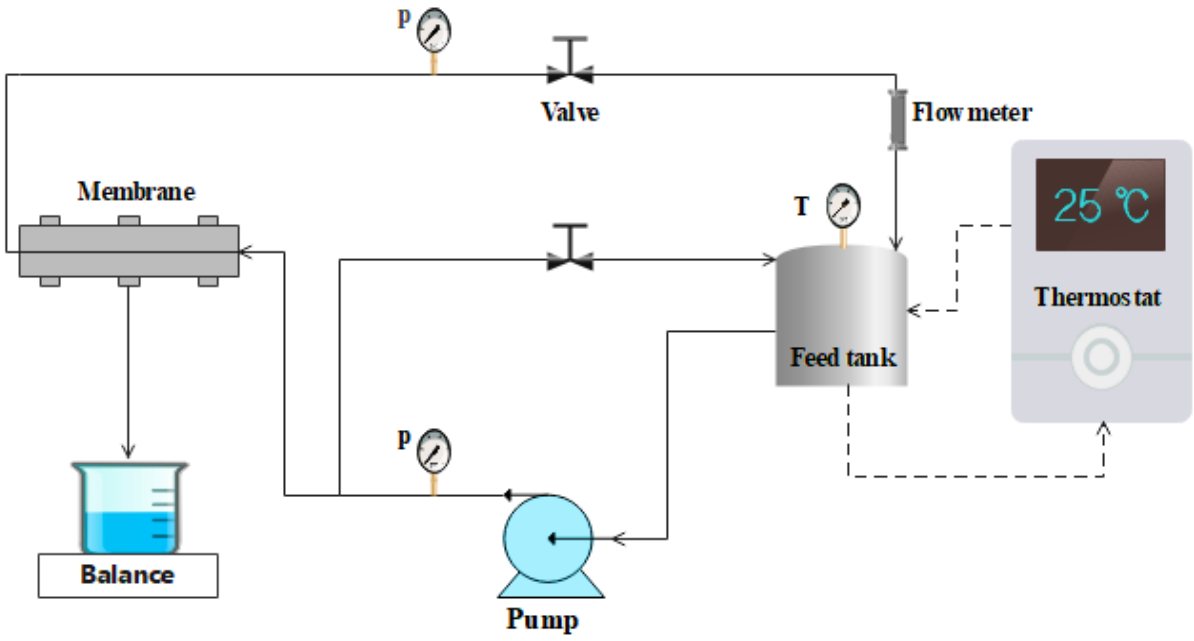

Figure 24. Experimental setup diagram, P pressure gauge, T temperature sensor.

5.2. Membranes

In this study, four different membranes were used Alfa lava, NF-Toray, NF270, and SELRO MPF-36; the characterization of these membranes are listed in **Table** 5-1.

Table 5-1 Membranes characterization.

Membrane	Manufacturer	Chemistry	MWCO (Da)	T range (°C)	P range (bar)	pH range
Alfa Laval	ALFA LAVAL	Polypiperazinamid Thin-film composite	300	5-60	15-40	1-12
NF-Toray	Toray	Polypiperazinamid Thin-film composite	200	50 ^{max}	55^{max}	2-11
NF270	FILM TEC	Polyamide Thin-film composite	200	45 ^{max}	41 ^{max}	2-11
SELRO MPF-36	Koch	Polysulfone Thin-film composite	1000	40-70	15-35	0-14

5.3. Chemicals

Lactic acid $CH_3CH(OH)COOH$ natural ≥ 85 %, Acetic acid CH3CO2H ≥ 99.8 %, D-(+)-Glucose $C_6H_{12}O_6$ ≥ 99.5 %, D-(−)-Fructose $C_6H_{12}O_6$ ≥ 99 % from Sigma-Aldrich company. Sodium chloride NaCl ≥ 99.5 % from fluka, Sodium sulfate Na_2SO_4 ≥ 99 % from Roth, Magnesium chloride $MgCl_2{\cdot}6H_2O$, Calcium chloride $CaCl_2$ from Reagenzein Merck, Potassium hydroxide KOH, and Ammonium chloride NH_4Cl were used to prepare the model solutions. The concentration of chemicals is listed in **Table 5-2**.

Table 5-2 Solutes concentration in the model solution

Solute	Concentration (g/L)
Lactic acid	25
Acetic acid	3,31
glucose	4,27
fructose	6,53
Na_2SO_4	0,23
$MgCl_2.6H_2O$	1,2
NaCl	1,2
$CaCl_2$	0,5
KOH	1
NH_4OH	1

The relevant characteristics of the organic solutes are listed in **Table 5-3**

Table 5-3 Principal characteristics of the investigated compounds.

Solute	Molecular formula	Molecular weight (g/ mol)	Diffusion coefficient at 25 °C (10^{-6}·cm2·s-1)	molecular radius r_s (nm)
Lactic acid	$CH_3CHOHCOOH$	90,08	9,96[b]	0,22[b]
Acetic acid	CH_3COOH	60,05	12,9[c]	0,19[c]
Glucose	$C_6H_{12}O_6$	180,1	6,73[a]	0,3156[a]
Fructose	$C_6H_{12}O_6$	180,1	6,80[a]	0,3235[a]

[a] from (Lei Yao et al. 2018), [b] from (Dey et al. 2012), [c] from (Weng et al. 2009)

5.4. Experimental procedure

The new membrane was first compacted by filtering deionized water at 32 bar for 20 min; then, the water permeability was measured. After that, the feed tank was filled with the solution to start the experiment. The process continued until the collection of approximately (1400 g) of permeate. Brix, conductivity, and pH in both permeate and retentate were measured during the process at a specific interval time; the permeate weight was also registered simultaneously. At the end of each experiment, the unit was cleansed 2-3 times with deionized water at the operating pressure and temperature; then, the water permeability was measured.

The flux was calculated with equation (5.1), where ΔM stands for the mass difference in a defined interval time (Δt), and A stands for the membrane area. The flux is often taken as a measurement of productivity.

$$J = \frac{\Delta M}{A\,\Delta t} = \left[\frac{Kg}{m^2\,h}\right] \tag{5.1}$$

The rejection of each solute, R, was determined through equation (5.2), where C_{Pi} and C_{Ri} represent the concentration of solute I of the permeate and retentate, respectively.

$$R = 1 - \frac{C_{P,i}}{C_{R,i}} \tag{5.2}$$

This procedure was applied to all experiments carried out in the framework of this study. All the experiments were performed at stable pressure (**32** bar) and categorized into two parts; the first part determines the optimal PH and temperature for LA separation. The experiments of the first part and their associated operating conditions are listed in **Table 5-4**

Table 5-4 Determining the optimal temperature and pH experiments

Experiment	Solution	Concentration ($g.L^{-1}$)		Temperature (°C)	pH	Pressure (bar)
Determining the optimal Temperature	LA	25		25	2.8	32
	LA	25		40	2.8	32
		LA	NaOH			
Determining the Optimal pH	LA + NaOH	25	3,5	25	3,8	32
	LA + NaOH	25	7	25	6	32

The second part of the experiments was carried out to study the effect of residual sugar in the solution model. The experiments of this part were performed under temperature 25 °C, pH 2,8, and pressure 32 bar. The used model solutions in these experiments are detailed in **Table 5-5**.

Table 5-5 Experiments for studying the effect of sugars on LA separation

Experiment	Solution	Concentration ($g.L^{-1}$)			
		Lactic acid	Acetic acid	Glucose	Fructose
1	Glucose	-	-	4,27	-
2	Fructose	-	-	-	6,53
3	Glucose +Fructose	-	-	4,27	6,53
4	LA + AA + GLU+ FRU + Salts (Model solution)	25	3,31	4,27	6,53
5	LA + AA + FRU+ Salts (Solution without glucose)	25	3,31	-	6,53
6	LA + AA + GLU + Salts (Solution without fructose)	25	3,31	4,27	-
7	LA + AA + Salts (Solution without sugars)	25	3,31	-	-

5.5. Analytical methods

5.5.1. Determination of pH and conductivity

The feed, permeate, and retentate's pH values were measured regularly using a WTW ADA S7/IDS pH electrode.

5.5.2. Refractive index (nD) and sugar concentration (°Brix) measurements

A.KRÜSS Optronic Digital Refractometers (Model KRÜSS_2007) was used to determine glucose and fructose concentration in the feed, retentate, and permeate samples (figure 5.3). The sugar concentration is measured in °Brix, and the refractive index nD was also determined. Refractometry is a method for determining how light is refracted as it travels through a particular material, an unknown molecule. The refractive index is determined by the amount by which light is refracted. The refractive index may be used to determine the identity of an unknown liquid chemical or to determine the purity of a liquid compound by comparing it to published values. The closer the refractive index value is to the values reported in the literature, the purer the sample. The refractive index is the ratio of light speed in the air to the light speed in the medium under consideration (Dr. Scott Chalmers 1998) as in Eq (5.3).

$$n_D = {}^{v_{air}}/_{v_{liquid}} \tag{5.3}$$

Figure 25. Digital Refractometer (A. KRÜSS Optronic).

A calibration curve was drawn between known solute concentration and Brix to determine glucose and fructose concentration in their single solution.

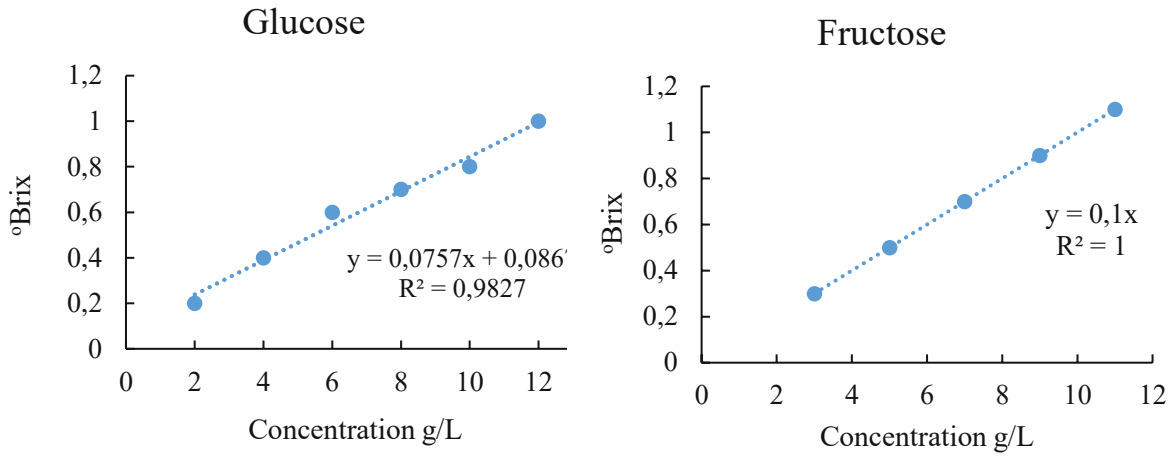

Figure 26. Calibration curve between Brix and concentration for glucose (left) and fructose (right)

5.5.3. Determination of organic solutes concentration

The concentration of LA, AA, fructose, and glucose in the retentate and permeate streams were determined by high-performance liquid chromatography (HPLC). Shimadzu Prominence 20 HPLC UFLC System (Figure 5) equipped with an autosampler (SIL-20A) including temperature control for the column (CTO-20AC), a refractive index (RI) detector (RID-10A), Shodex sugar SH1011 column (8 × 300 mm). The column temperature was set to 50 °C. The mobile phase was (5 mM) sulfuric acid at a flow rate of (0,6 mL.min^{-1}). Each sample's injection volume was (10 µL). All samples were diluted by two dilution factors of eight and two with deionized water. Due to high lactic acid concentrations, a dilution factor of 1:8 was applied. In comparison, acetic acid, glucose, and fructose were in trace amounts; thus, a factor of 1: was applied for dilution.

Individual LA, AA, glucose, and fructose were identified by comparing retention times with authentic standards. Their concentrations were determined by the standard external method. For this purpose, standard solutions of LA, AA, glucose, and fructose, were prepared at four concentrations to create calibration curves for the HPLC analysis. Calibration graphs were produced for each component using peak areas versus analyte concentration.

Figure 27. Shimadzu Prominence 20 HPLC UFLC System.

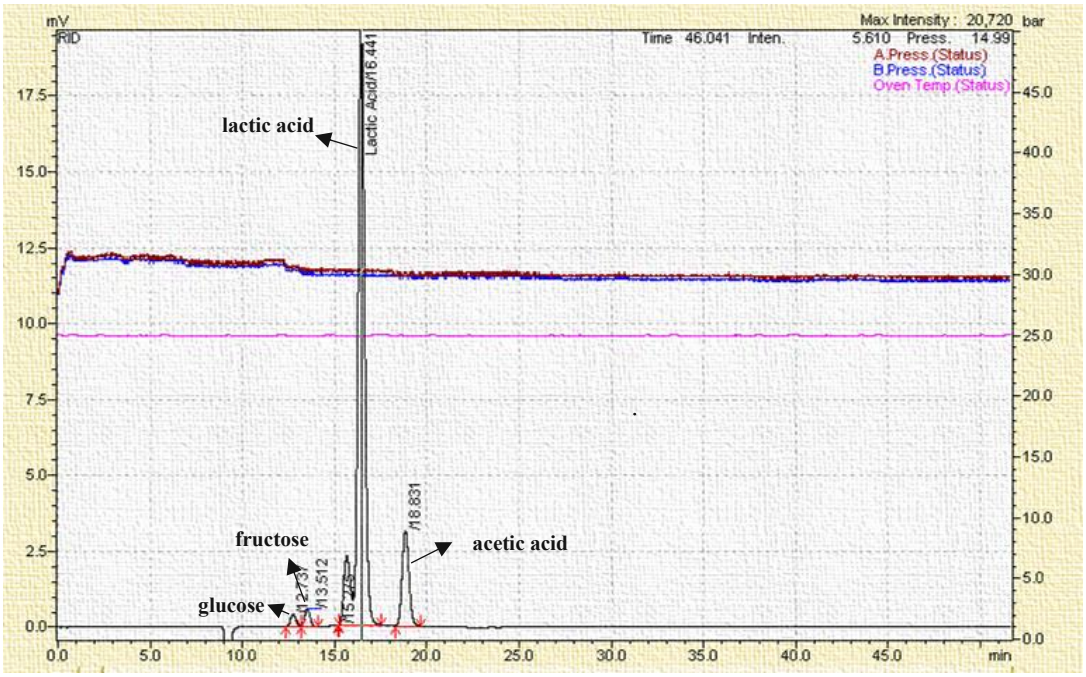

Figure 28. HPLC result for the detection of lactic acid, acetic acid, glucose, and fructose

6.Results and Discussion

6.1. The effect of operating conditions on the membrane separation performance

In this section, the effect of operating parameters specifically, temperature and pH, on the transport of LA through the membranes will be presented. The optimal pH and temperature will be adopted for the following experimental approach depending on a compromise between two main factors: the rejection of lactic acid and permeate flux.

6.1.1. The effect of temperature

The effect of temperature on the rejection of LA is illustrated in **Figure 29**. It shows that the operating temperature alters the retention of LA in diverse commercial membranes differently. The rejection of LA increased with increasing the temperature from 25 °C to 40 °C for three membranes, Alfa Laval NF, NF-Toray, and SELRO MPF-36. At higher temperatures, the solvent's viscosity decreased, leading to water passing more easily through the membrane, resulting in lower solute concentration in the permeate and higher solute retention. While in NF270, the rejection slightly decreased from 71 % at 25 °C to 64 % at 40 °C; this is attributed to the expansion of the membrane pore radius as the temperature increases; also, the ability of higher temperatures to alter the pores density of the NF270 membrane could increase the permeate flux of LA according to (Dang et al. 2014).

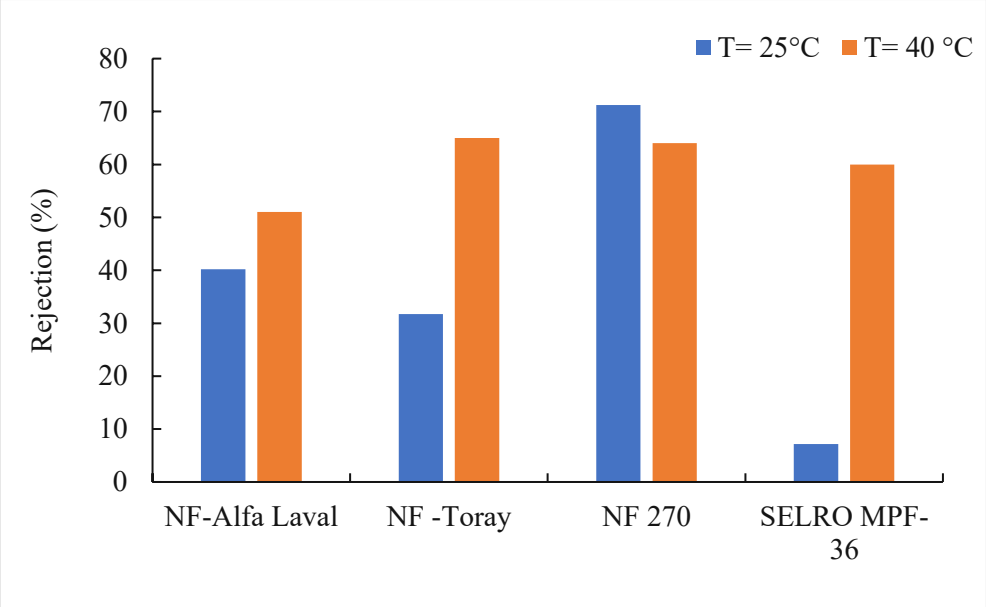

Figure 29. Rejection of lactic acid at 25 °C and 40 °C

It is worth mentioning that MPF-36 achieved the lowest rejection of LA at 25 °C, due to its high MWCO compared to other membranes; however, the increase in temperature considerably increased the rejection of LA

The effect of temperature on permeate flux is illustrated in **Figure 30**. All membranes showed higher flux with increasing the temperature, which has been attributed to the decrease in water viscosity from 0,89 to 0,652 (mPa.s) as the temperature increased from 25 °C to 40 °C

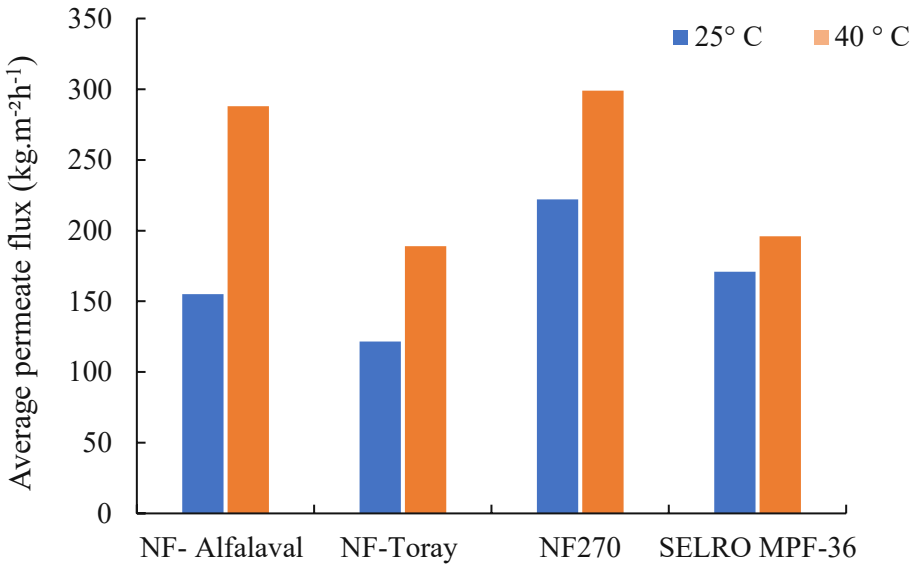

Figure 30. Permeate flux at 25 °C and 40 °C.

As shown in **Figure 31**, no water flux reduction was observed during the experiments at both operating temperatures, as the average water flux before and after filtration did not change considerably**.**

The highest decrease in water flux at 25 °C was observed in NF-270 as the flux decreased about 10 % after filtration. Meanwhile, at 40 °C, the reduction in pure water flux after filtration was about 13% in SELRO MPF -36

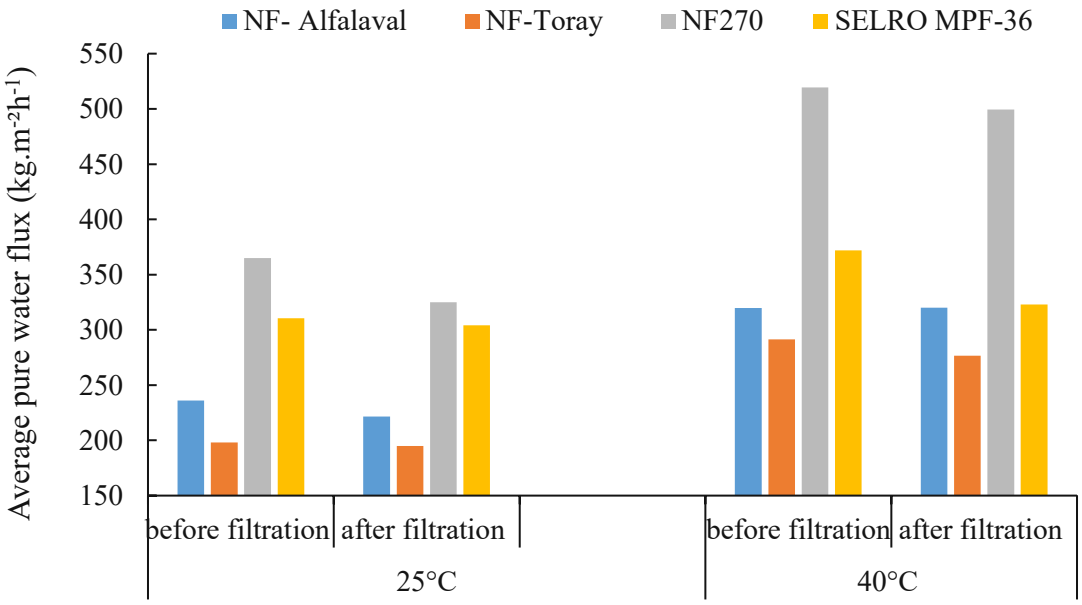

Figure 31. Average pure water flux before and after filtration at 25 °C and 40 °C.

6.1.2. The effect of pH

The rejection of LA variation with pH is presented in **Figure 32**. It is observed that the rejection increased with increasing the pH for all membranes. The reason for that is, when pH is low, LA is undissociated, and the Donnan effect is neglected; the only mechanism of molecular rejection is steric exclusion, which means that the molecules are retained only by their size. As pH increase, the acid is deprotonated, and the membranes tend to have negative surface charges. Thus, electrostatic repulsion between the membrane surface and dissociated acid (negatively charged) is enhanced, which causes higher LA rejection.

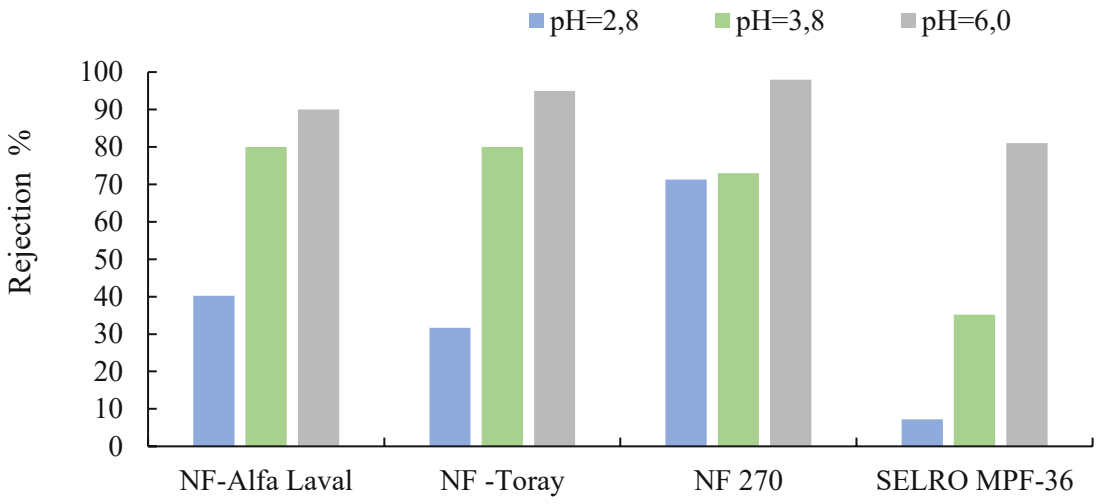

Figure 32. The rejection of LA as a function of pH.

The permeate flux variations with pH are illustrated in

Figure *33*; the permeate decreases with high pH for all membranes. That is because of an increase in the number of species due to acid dissociation and the formation of sodium lactate. According to Tang et al. 2008, as the pH in the feed decreases, amino groups on the membrane surface are changed into RH_3N^+ or R_3HN^+, which causes an increase in the hydrophilicity of the membrane and enlarged membrane pores. As pH gets higher electrostatic repulsion between the negatively charged $-COO^-$ group on the membrane surface and OH^- in the feed solution causes shrinkage of the pores.

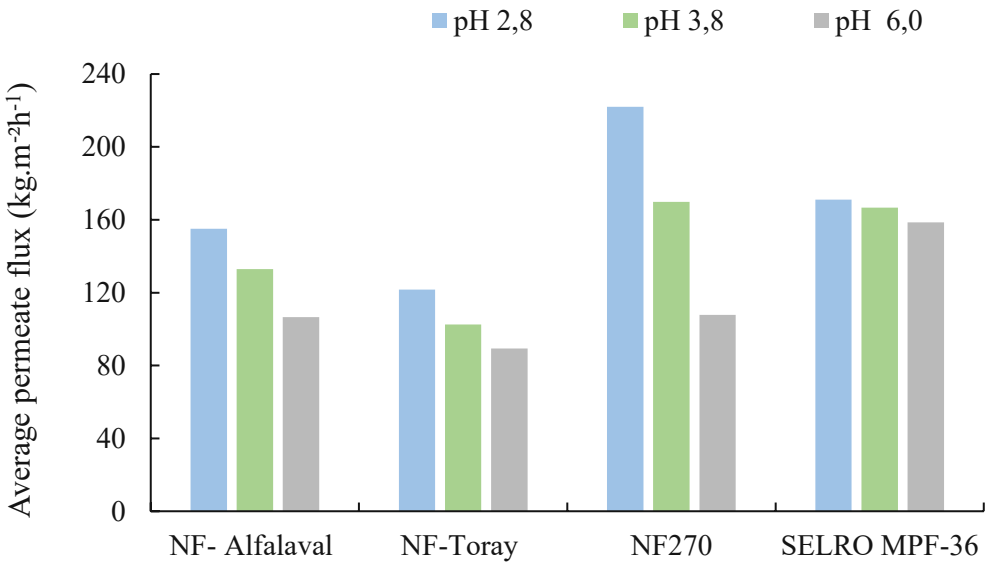

Figure 33. Average permeate flux at different pH.

The average pure water flux before and after filtration did not indicate serious reduction. However, (Nanda et al. 2010) studied the effect of pH on the membrane fouling and concluded that fouling potential increases with increasing acidity of the feed solution. In acidic conditions, a sticky foulant layer was formed on the membrane surface compared to a relatively loose deposit for a feed solution with pH 7,5.

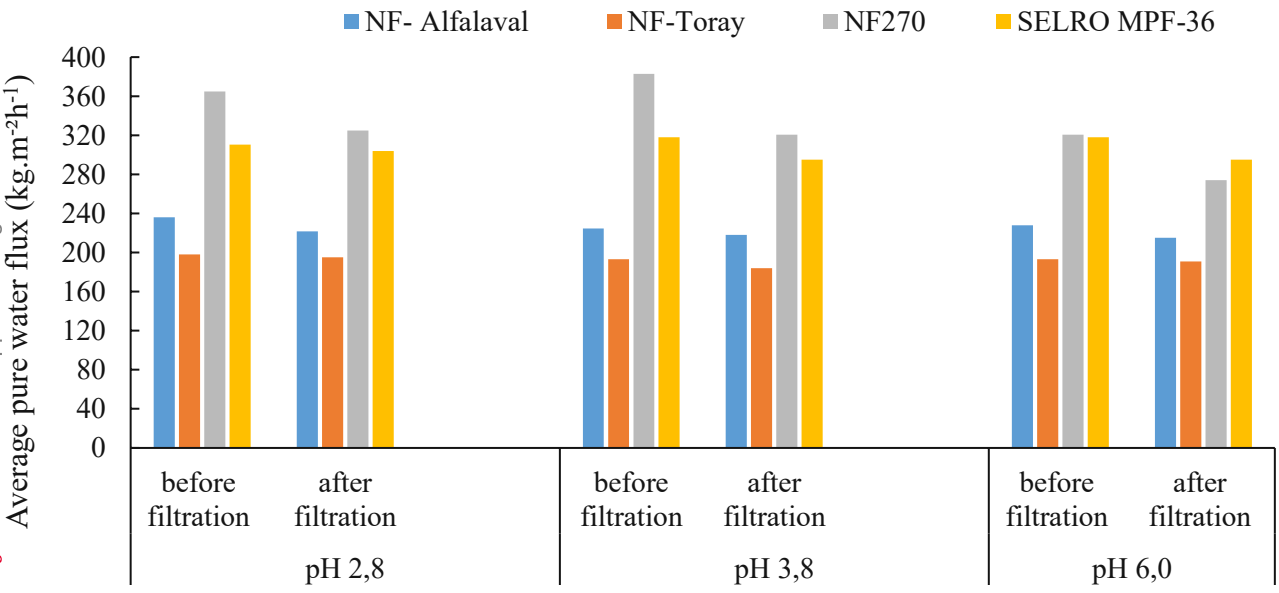

Figure 34. Average Pure water flux before and after filtration at different pH.

depending on these results, the temperature of 25 °C and pH of 2,8 has been adopted for the following experiment's approach

6.2. Separation of sugar solutions

The rejection of a single glucose solution, a single Fructose solution, and a mixed solution containing both fructose and glucose will be discussed in this section. It is essential to understand the performance of membranes with the individual solutions and how the performance changes with binary solution (glucose and fructose) and the matrix solution (LA, AA, Salts, Fructose, Glucose).

The rejection data of individual solutions can be used furthermore to determine membrane properties for fructose and glucose, such as hindrance factor for convection (K_c), effective pore radius (r_p), and thickness-porosity ratio ($\Delta x/Ak$), for modeling purposes.

Glucose and fructose are neutral solutes in the aqueous solution; hence the separation mechanism of both neutral molecules is mainly based on the size exclusion, and membrane charge can be neglected.

Membrane performance in the separation of both glucose and fructose in their individual solution is illustrated in **Figure 35** and **Figure 36**. Membranes with low MWCO, Alfa Laval (300 Da), NF-Toray (200 Da), and NF270 (200 Da) can reject almost 100 % of glucose and fructose. However, SELRO MPF-36 did not achieve the highest rejection of glucose and fructose, with a 50 % and 70 %, respectively, due to its relatively high MWCO (1000 Da).

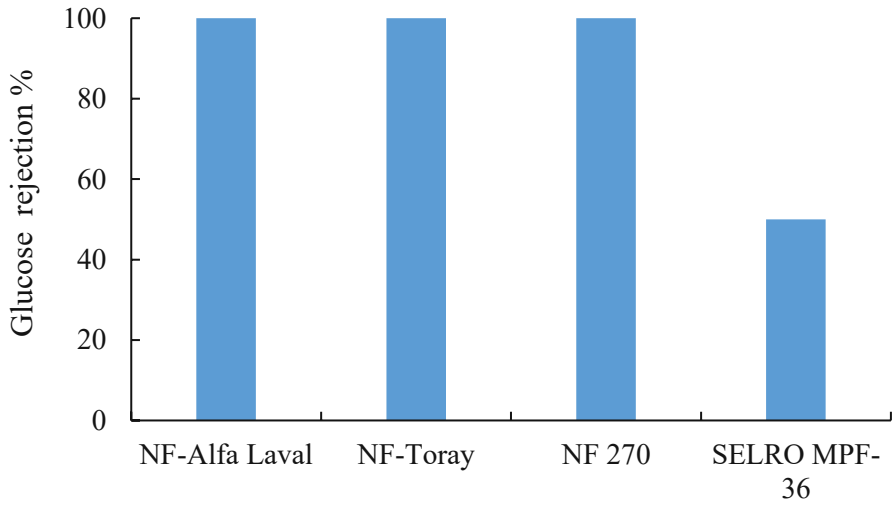

Figure 35. Glucose rejection in individual solution.

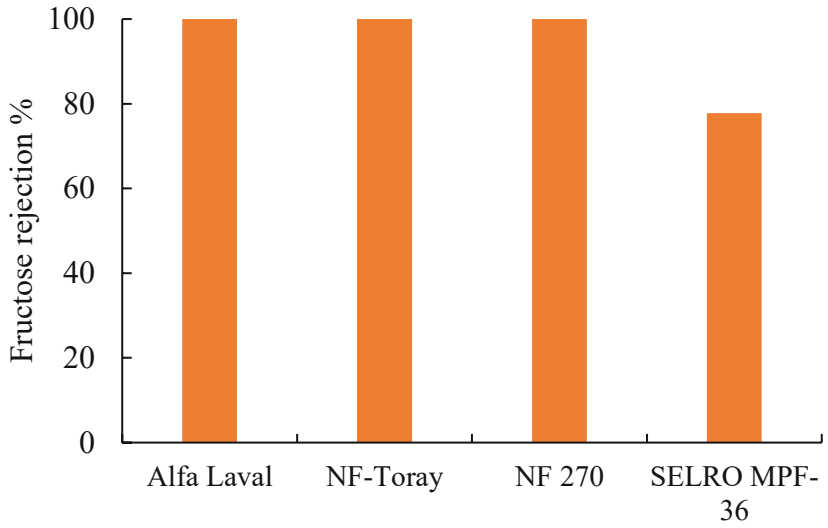

Figure 36. Fructose rejection in individual solution.

In the case of binary solution (glucose + fructose) shown in **Figure 37**, the rejection of glucose was slightly decreased for low MWCO membranes, whereas the rejection of fructose did not change for the same membranes. The main change was detected with the SELROMPF-36 membrane as the rejection of both glucose and fructose was dramatically decreased to 16,9 % and 17,4 %, respectively. It may be explained that the presence of both fructose and glucose increases the viscosity of the solution, which greater quantities of the solutes accumulation at the membrane surface, thereby leading to severe concentration polarization. Thus, solute diffusion through the membrane would be enhanced, resulting in decreased solutes retention.

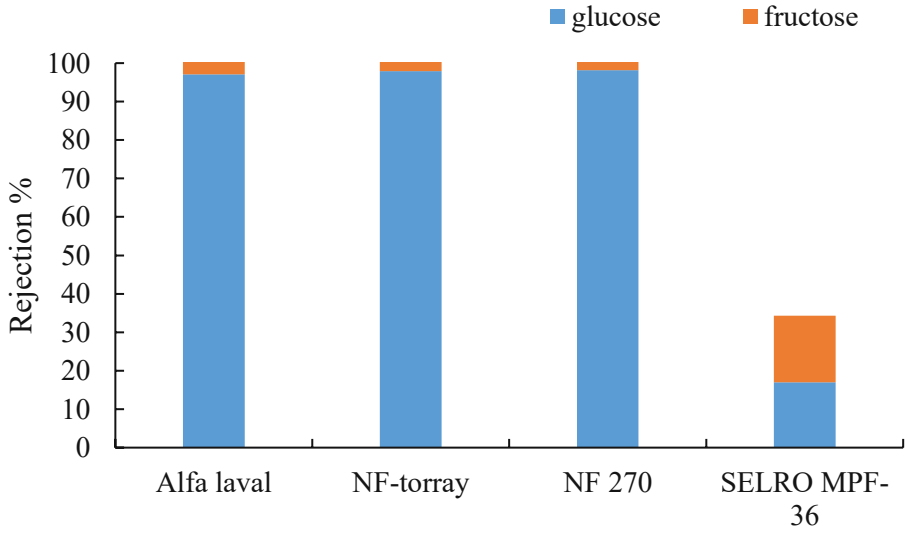

Figure 37. Separation performance of mixture solution (glucose +fructose)

6.3. The effect of sugar on LA separation

Four solutions of different compounds were prepared. The standard solution with a composition of (LA + AA + Salts + Glucose + Fructose), the solution without fructose, the solution without glucose, and the solution without sugars were tested to study the effect of sugar on the rejection of LA. In these trials, membranes with different MWCO and made of different polymers substrates were used, as mentioned in **Table** 5-1. The performance of each membrane regarding the rejection of LA, Sugar, and AA with these different solutions will be discussed as follow.

6.3.1. Alfa Laval performance

The LA rejection and permeate flux variations versus different solutions are plotted in **Figure 38**. In the case of the model solution, the rejection of LA is about 58,6 %. However, the rejection increased to 64 % in the absence of sugars from the feed solution, which indicates the positive effect of sugar's presence on the LA separation. Here, the high osmotic pressure of glucose and fructose combination reduces the net driving force available for water molecules' convection and increases the solute flux; therefore, the LA concentration in permeate will be higher.

The presence of glucose alone (solution without fructose, experiment 6 in **Table 5-5**) decreased the rejection of LA slightly compared to the standard solution by about 57,9 %; here, the osmosis effect decreased as the feed solution contains only glucose with a minor concentration 4,27 g/L.

In the contract to glucose, the effect of fructose was considerable, as it reduced the rejection of LA. This positive effect of fructose may be attributed to the higher efficiency in osmosis, according to (Darwish et al. 2014).

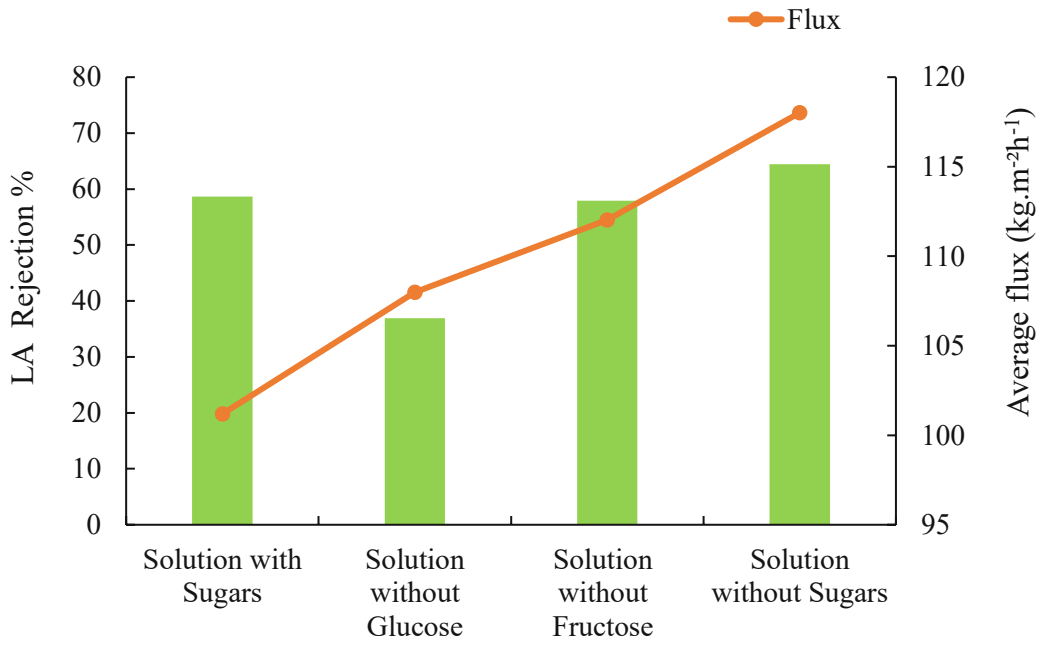

Figure 38. LA rejection and permeate flux as a function of solution composition (Alfa Laval).

The average permeate flux clearly explains the effect of sugar solutions' osmotic pressure. The feed solution with both fructose and glucose has the highest osmotic pressure, reflected in the decrease of the permeate flux. Higher osmotic pressure causes higher back diffusion of solvent, and the flux increase with decreasing the osmosis effect, as is shown in **Figure 38**

Alfa Laval achieved high rejection of sugars, as it is shown in **Figure 39**, the varying of solution composition did not affect the high rejection of sugars

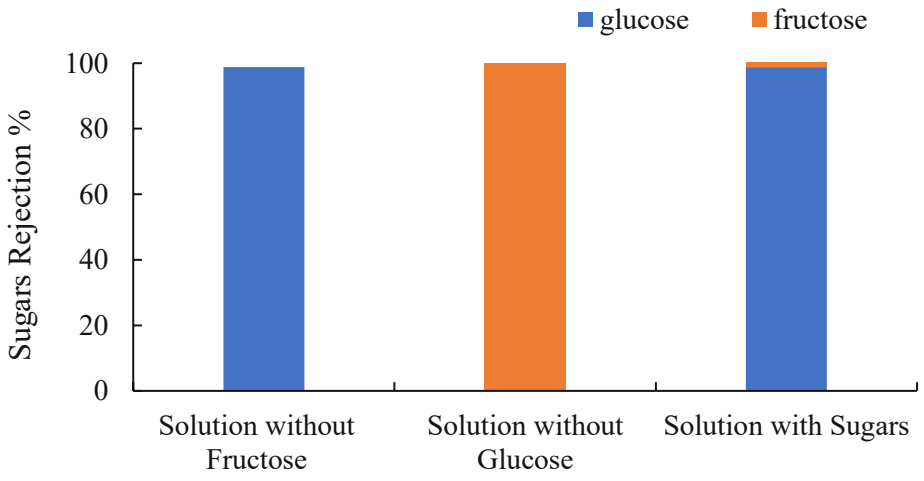

Figure 39. Sugar rejection as a function of solution composition (Alfa Laval)

The effect of sugars on AA rejection in Alfa Laval is illustrated in **Figure 40**. due to the small molecular weight of AA as mentioned in **Table 5-3**, compared to other organic solutes in model solution, it is less sterically hindered during membrane permeation; hence AA is less rejected than LA. The presence of fructose alone in feed solution (solution without glucose) decreased the rejection of AA greatly as negative rejection was observed about – 15 %, which indicates high enrichment of AA in permeate side compared with the rejection side. Meanwhile, glucose increased the rejection of AA to about 15%. The highest rejection was observed with feed solution without sugars, about 33 %.

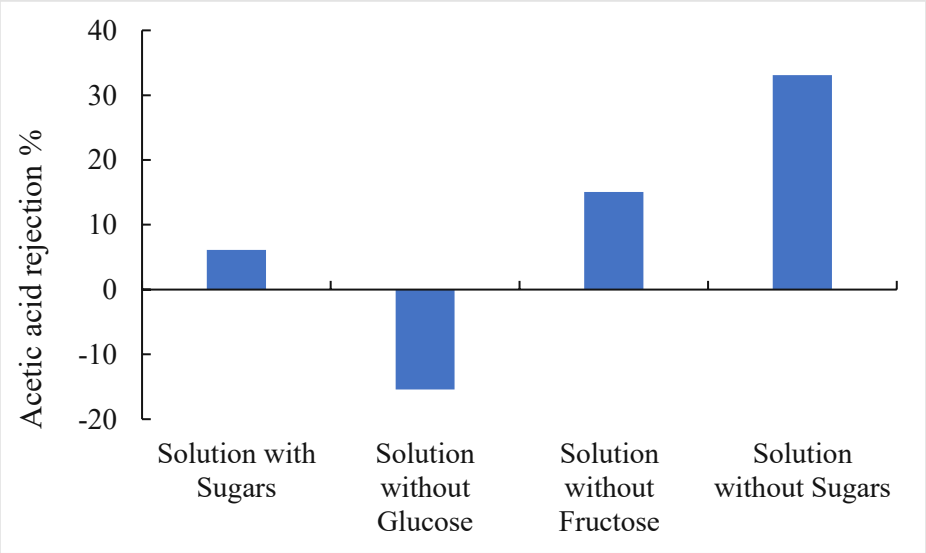

Figure 40. AA rejection as a function of solution composition (Alfa Laval).

6.3.2. NF-Toray performance

Figure 41 shows the rejection of LA in NF-Toray; from the plot, it is clear that the rejection for all solutions containing sugars is very high; removing glucose or fructose from feed solution did not change the transport behavior of LA. This may be due to the low MWCO of the membrane and the high affinity between sugars and selective layer (poly piperazine amid) of the membrane, which leads to the accumulation of sugar on the membrane surface and forming a barrier preventing LA from flowing across the membrane. The lowest rejection was observed when the feed solution did not contain glucose and fructose (solution without sugars)

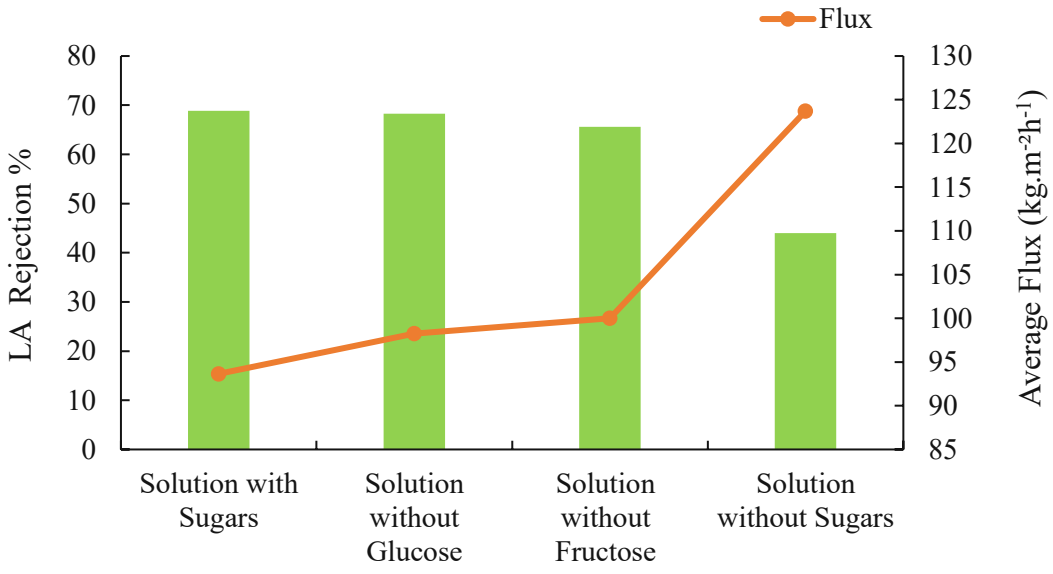

Figure 41. LA rejection and permeate flux as a function of solution composition (NF-Toray)

The permeate flux in NF-Toray for all solutions containing sugars is the lowest compared to other employed membranes. The permeate fluxes were of the order, solution without sugars > solution without fructose > solution without glucose > solution with sugars. Low flux implies a high osmosis effect.

Figure 42 presents the sugar rejection as a function of the solution composition. NF-Toray can effectively reject almost 100% of sugars.

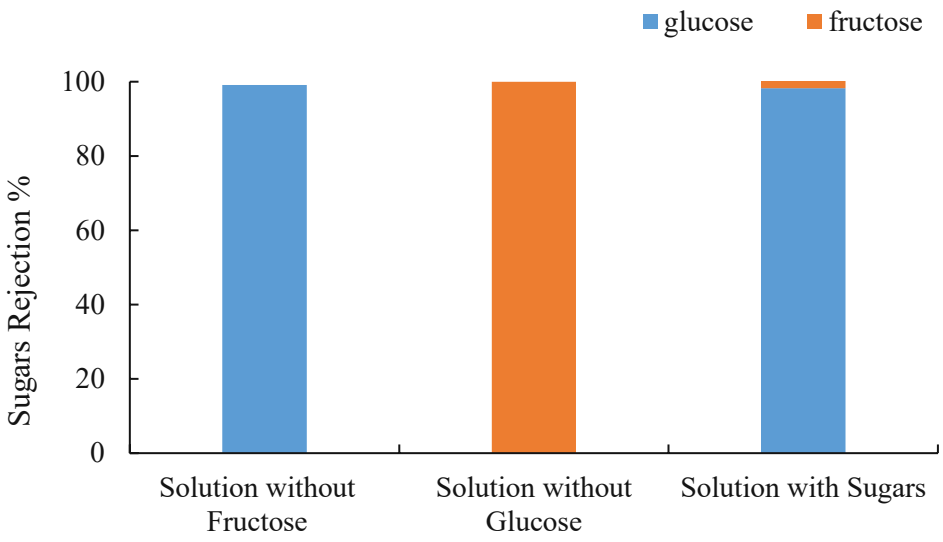

Figure 42.Sugar rejection as a function of solution composition (NF-Toray)

NF-Toray rejects acetic acid at the highest value when the feed solution contains glucose and fructose. In contrast to other membranes, glucose alone (solution without fructose) decreases the rejection to about 13 %, while the rejection is higher in the case of a solution containing only fructose (solution without glucose), as shown in **Figure 43**

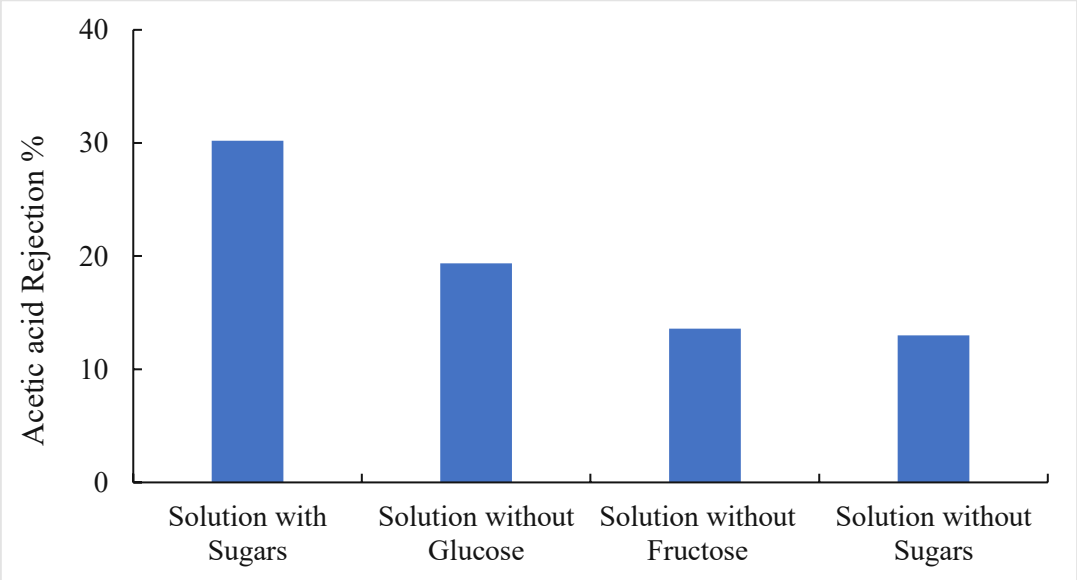

Figure 43. AA rejection as a function of solution composition (NF-Toray).

6.3.3. NF270 performance

Figure 44 shows the NF270 performance regarding LA rejection and the average permeate flux for each solution. The rejection value for feed solution with glucose and fructose is 61%; this value increases with removing glucose and fructose from the feed solution. This behavior is because the osmosis effect is significantly reduced by removing the draw solutes (glucose and fructose). The rejection decreased in the case of a solution containing only fructose (solution without glucose); this happened most likely, due to the high osmosis effect of fructose. Whereas the rejection increased considerably with the presence of glucose alone in the feed solution, even higher than the standard solution, that can be explained by the previous study of (Lei Yao et al. 2018), the study concluded that glucose has a higher affinity to the Polyamide (the selective layer of NF270). Due to the small pore size of the membrane, glucose could partly block the membrane's pores, leading to a higher rejection of LA.

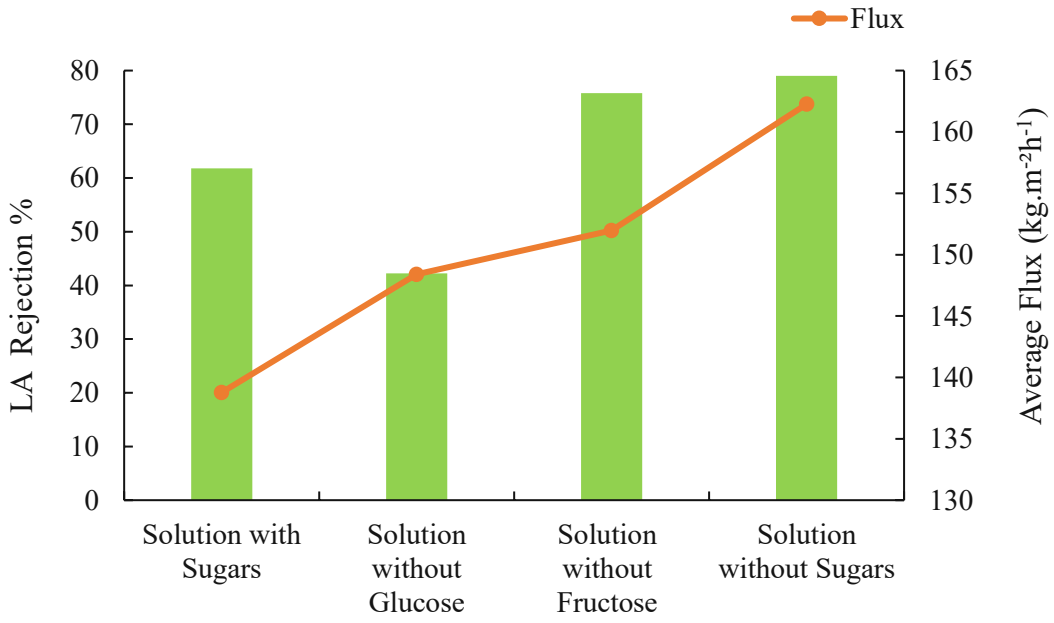

Figure 44. LA rejection and permeate flux as a function of solution composition (NF270)

High permeate flux was recognized with NF-270 compared to other employed membranes, and the flux also decreased with the presence of sugars (draw solutes). The sequences of average permeate flux of the solutions were solution without sugars > solution without fructose > solution without glucose > solution with sugars.

Figure 45 shows the rejection of sugar versus solution composition, NF270 reject glucose and fructose by 100 %

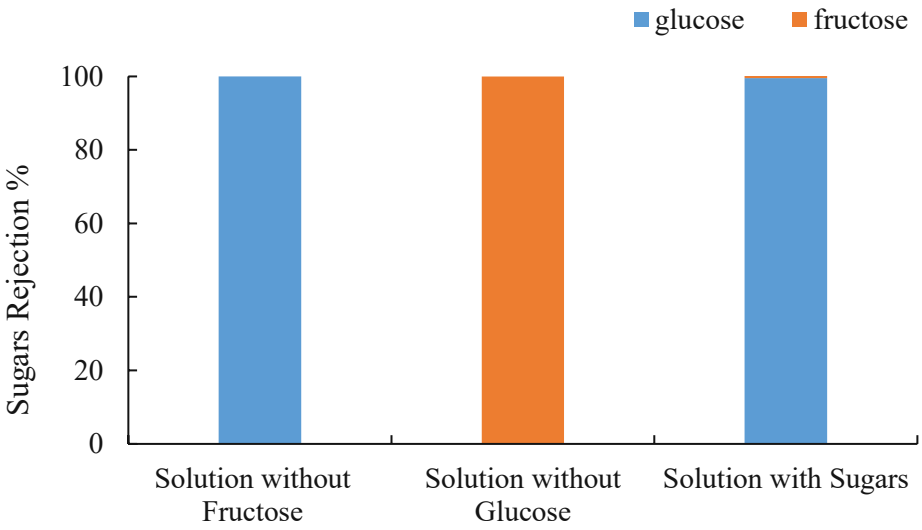

Figure 45. Sugar rejection as a function of solution composition (NF270)

The highest rejection of AA was achieved with NF270 membrane in the case of filtering feed solution without sugars about 52 %. When feed solution containing only glucose (solution without fructose) a rejection of 44 % was observed. In contrast, the presence of fructose alone decreases the rejection greatly to a negative value of – 42 %, as shown in **Figure 46**.

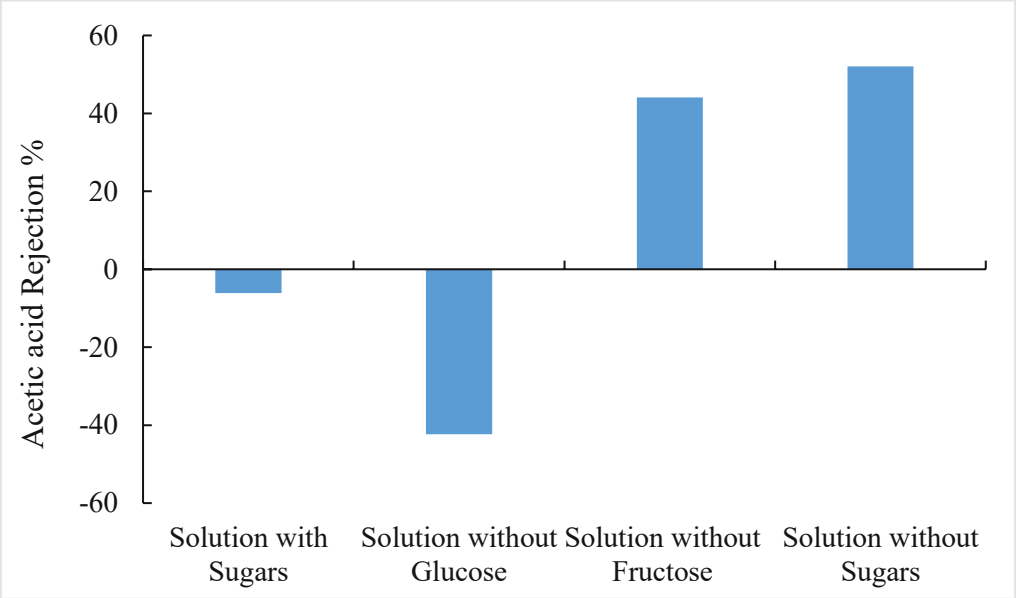

Figure 46. AA rejection as a function of solution composition (NF270).

6.3.4. SELRO MPF-36 performance

The behavior of LA rejection as a function of solution composition is shown in **Figure 47**. The rejection of LA has the lowest value compared to other membranes, and it is almost the same for feed solutions with sugar and without sugar. Due to its high MWCO (1000 Da), the membrane allows the sugar partially to pass through, which decreases the effect of osmotic pressure, whereas the presence of fructose alone without glucose decrease the LA rejection. However, the highest rejection was observed when the feed solution contained only glucose.

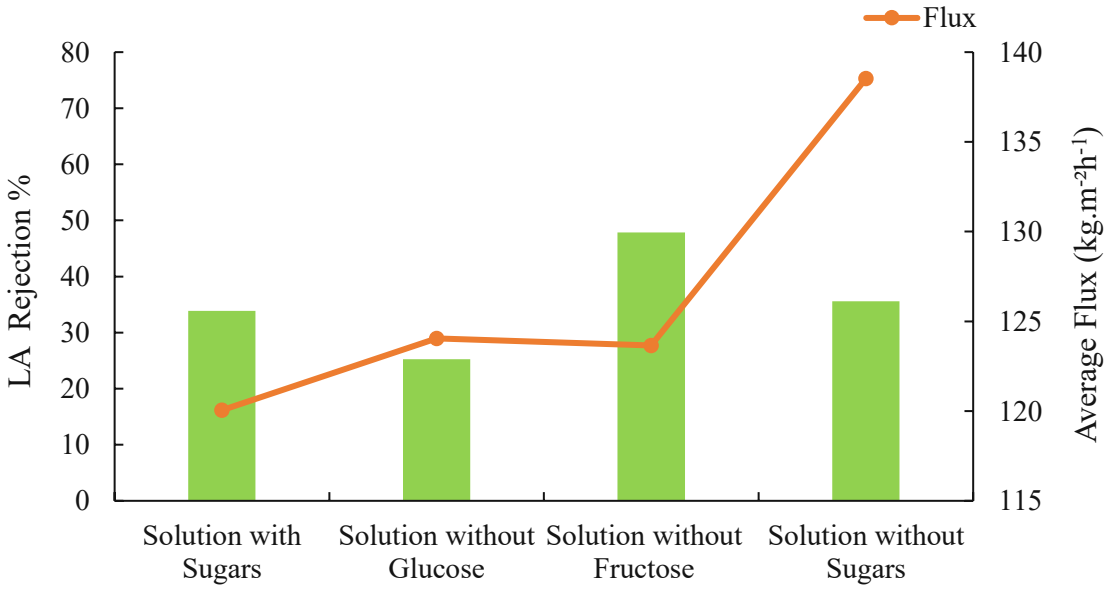

Figure 47. LA rejection and permeate flux as a function of solution composition (SELRO MPF-36)

As shown in **Figure 48**, SELRO MPF-36 did not achieve high sugar rejection due to its high MWCO, which is considered a drawback of this membrane, despite the low rejection of LA.

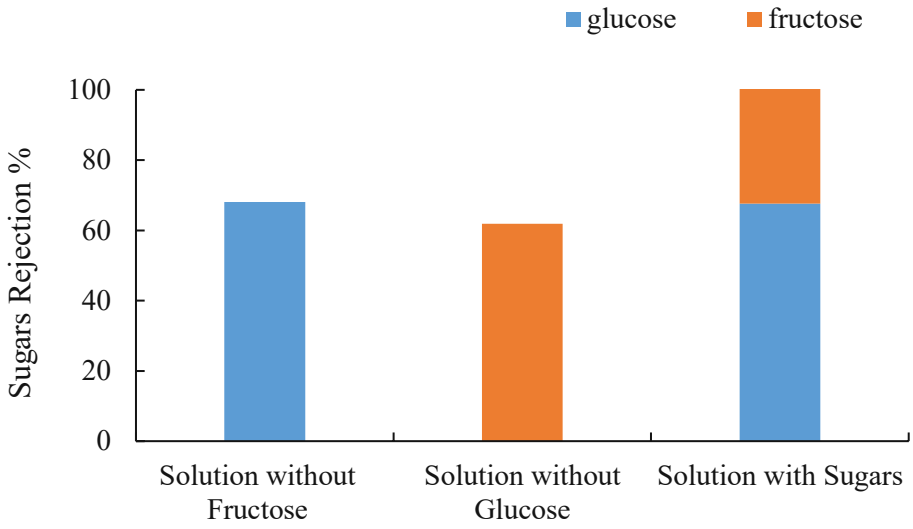

Figure 48. LA rejection and permeate flux as a function of solution composition (SELRO MPF-36).

A negative rejection value of AA was observed for all solutions except solution without fructose. This negative value increased considerably to about -37 % with the filtrating solution containing fructose, which indicates that fructose has a positive effect on permeating AA through the membrane, unlike the presence of glucose alone in the feed solution, as it raised the rejection to a positive value of about 3,5%

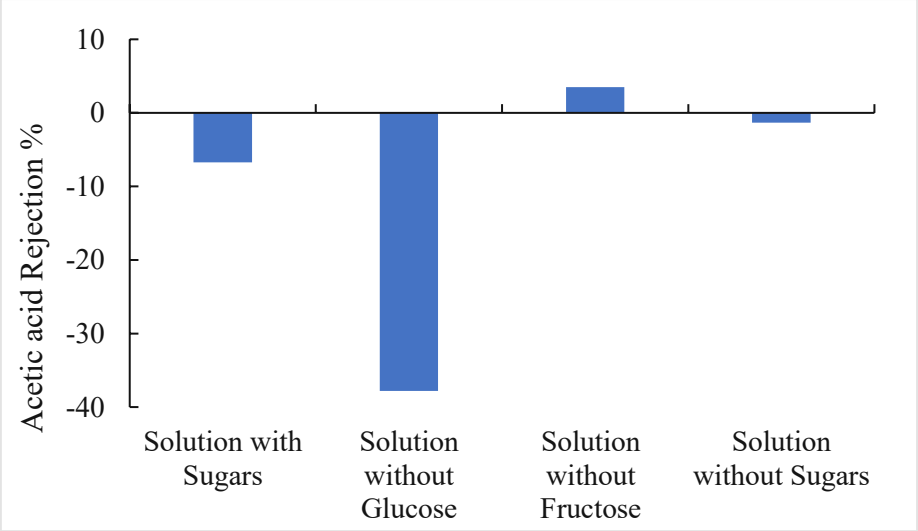

Figure 49. AA rejection as a function of solution composition (SELRO MPF-36).

6.3.5. Comparative assessment of the sugar effect on LA rejection between employed membranes

Figure 50 present the LA rejection variation versus model solution composition. It is clear that glucose and fructose differently impact the rejection of LA; this effect can be positive or negative depending on the membrane material and MWCO, but in general, the presence of fructose in the model solution decreases the LA rejection. In contrast, glucose has a negative effect as it increases LA rejection.

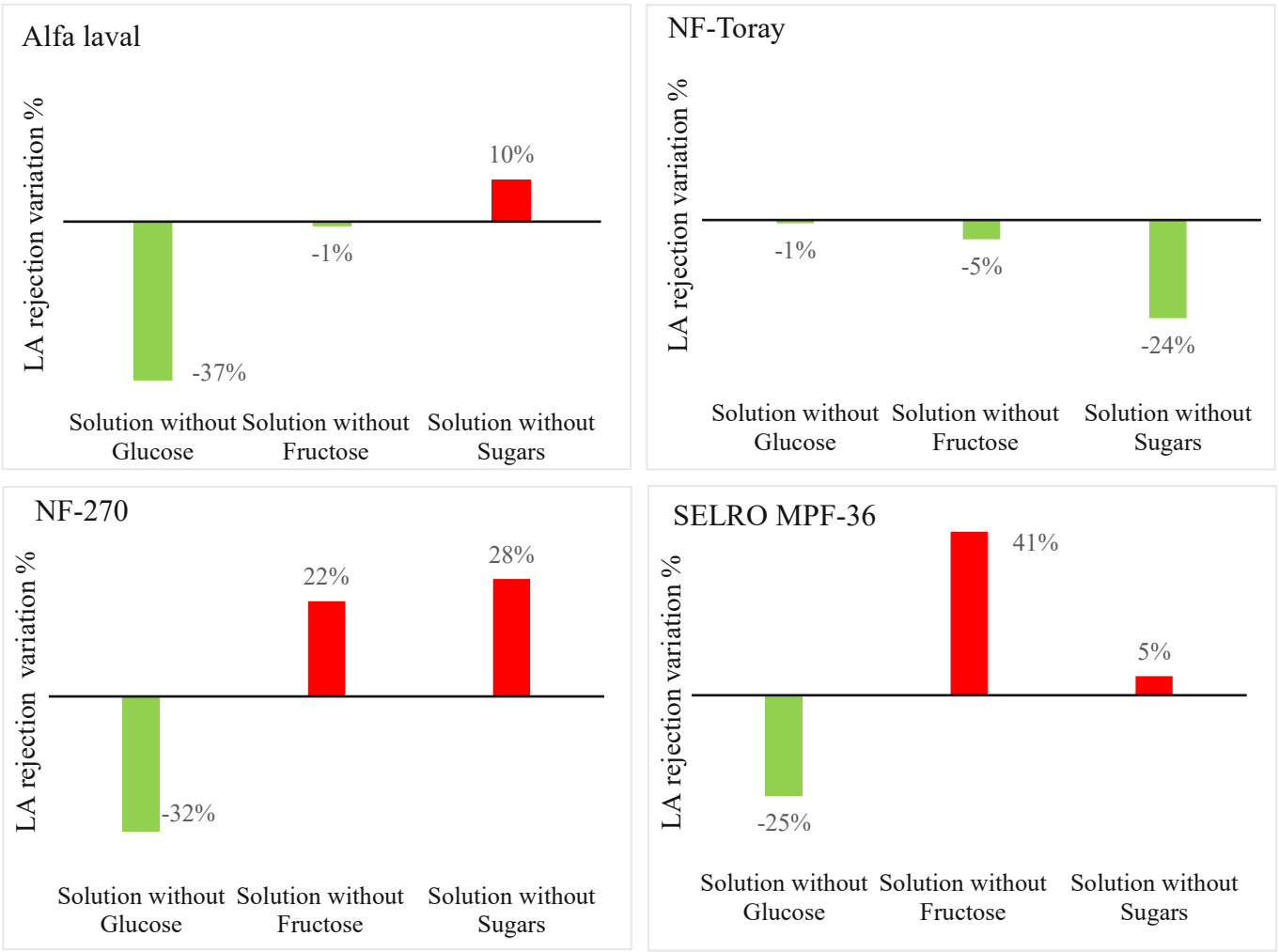

Figure 50. Relative variation of LA rejection.

7.Summary and Conclusion

In this work, experiments were carried out to investigate the effect of operating parameters and the effect of residual sugars in the feed solution on the separation of LA via NF. For this purpose, four commercial membranes with different MWCO and different materials were employed (Alfa Laval , NF-Toray, NF270, and SELRO MPF-36)

The operating parameter effect investigation was carried out with a single system (Deionized water + Lactic acid) to determine the optimal temperature and pH for High LA yield on the permeate side. The conclusions that can be drawn from these experiments are summarized below:

- increasing the temperature from 25 to 40 °C increased the LA rejection for all membranes except NF-270. an increase in the permeate flux associated with an increase in temperature is mainly because of higher water transport but not LA
- Increasing the pH value of the feed solution causes higher rejection of LA due to the dissociation of LA to Lactate as the pH increases. The membranes also tend to hold a negative charge with increasing the pH, which causes electrostatic repulsion between Lactate and membrane.

The investigation of the residual sugar effect was carried out with a complex system (LA, AA, salts, glucose, and fructose). The composition was changed by removing glucose once, then removing fructose, and removing both from the model solution to determine how much the sugar composition could affect the LA rejection. The concluding remarks are summarized below.

A high increase in LA rejection was observed with the solution containing only glucose, especially for NF-270 and SELRO MPF-36 membranes. In contrast, for NF-Toray and Alfa Laval, the rejection slightly decreased about 5% and 1%, respectively, which denotes that glucose contributes to impeding acid transport through the membrane. the presence of glucose also enhanced a bit the rejection of AA; the highest rejection was observed with NF270 about 44%

the presence of fructose alone significantly improved the separation of LA; the rejection decreased remarkably for all the membranes, except NF-Toray. At the same time, negative rejection of AA was observed, which implies that fructose enhances the transport of both AA and LA

the absence of fructose and glucose did not improve the yield of LA, in the contract, the rejection of LA increased for all membranes. The same rejection pattern of AA was observed for all membranes except SELRO MPF-36

All the membranes achieved high rejection of sugars about 100%, except SELRO MPF-36 due to its high MWCO

These observations strongly imply that molecular sieving is not necessarily the only mechanism that controls the separation of LA. Other factors such as membranes morphology specification, solution composition, solute–solute interaction, and solute-membrane affinity can affect the separation of LA.

8. References

1. Agboola, Oluranti; Maree, Jannie; Kolesnikov, Andrei; Mbaya, Richard; Sadiku, Rotimi (2015): Theoretical performance of nanofiltration membranes for wastewater treatment. In: *Environ Chem Lett* 13 (1), S. 37–47. DOI: 10.1007/s10311-014-0486-y.
2. Ahmad, Ashfaq; Banat, Fawzi; Taher, Hanifa (2020): A review on the lactic acid fermentation from low-cost renewable materials: Recent developments and challenges. In: *Environmental Technology & Innovation* 20, S. 101138. DOI: 10.1016/j.eti.2020.101138.
3. Ahmad, Ashfaq; Othman, Israa; Taher, Hanifa; Banat, Fawzi (2021): Lactic acid recovery from date pulp waste fermentation broth by ions exchange resins. In: *Environmental Technology & Innovation* 22, S. 101438. DOI: 10.1016/j.eti.2021.101438.
4. Alves de Oliveira, Regiane; Alexandri, Maria; Komesu, Andrea; Venus, Joachim; Vaz Rossell, Carlos Eduardo; Maciel Filho, Rubens (2020): Current Advances in Separation and Purification of Second-Generation Lactic Acid. In: *Separation & Purification Reviews* 49 (2), S. 159–175. DOI: 10.1080/15422119.2019.1590412.
5. Alves de Oliveira, Regiane; Komesu, Andrea; Vaz Rossell, Carlos Eduardo; Maciel Filho, Rubens (2018a): Challenges and opportunities in lactic acid bioprocess design—From economic to production aspects. In: *Biochemical Engineering Journal* 133, S. 219–239. DOI: 10.1016/j.bej.2018.03.003.
6. Alves de Oliveira et al. (2018b): Challenges and opportunities in lactic acid bioprocess design From economic to production aspects. In: *Biochemical Engineering Journal* 133, S. 219–239. DOI: 10.1016/j.bej.2018.03.003.
7. Ang, W. L.; Mohammad, A. W. (2015): Mathematical modeling of membrane operations for water treatment, S. 379–407. DOI: 10.1016/B978-1-78242-121-4.00012-5.
8. Auras, Rafael; Lim, Loong-Tak; Selke, Susan E. M.; Tsuji, Hideto (Hg.) (2010): Poly(lactic acid). Synthesis, structures, properties, processing, and applications. Hoboken, N.J: Wiley (Wiley series on polymer engineering and technology).
9. Baker, Richard W. (Hg.) (2012): Membrane technology and applications. 3rd ed. Chichester West Sussex, Hoboken: John Wiley & Sons.
10. Beschkov, Venko N.; Yankov, Dragomir (Hg.) (2021): Downstream processing in biotechnology. Boston: De Gruyter.
11. Bharathiraja, B.; Chakravarthy, M.; Ranjith Kumar, R.; Jayamuthunagai, J.; Praveen Kumar, R. (Hg.) (2016): Integrated Biorefinery for Bioenergy and Platform Chemicals. Online verfügbar unter www.sciencedirect.com/science/article/pii/B9780128029800000225.
12. Bichot, Aurélie; Delgenès, Jean-Philippe; Méchin, Valérie; Carrère, Hélène; Bernet, Nicolas; García-Bernet, Diana (2018): Understanding biomass recalcitrance in grasses for their efficient utilization as biorefinery feedstock. In: *Rev Environ Sci Biotechnol* 17 (4), S. 707–748. DOI: 10.1007/s11157-018-9485-y.

13. Bisaria, Virendra S. (2014): Bioprocessing of Renewable Resources to Commodity Bioproducts. DOI: 10.1002/9781118845394.

14. Brandt, Agnieszka; Gräsvik, John; Hallett, Jason P.; Welton, Tom (2013): Deconstruction of lignocellulosic biomass with ionic liquids. In: *Green Chem.* 15 (3), S. 550. DOI: 10.1039/c2gc36364j.

15. Chong, Tzyy Haur; Fane, Anthony G. (2021): Nanofiltration Module Design and Operation. 3. In: Nanofiltration: John Wiley & Sons, Ltd, S. 95–135.

16. Cui, Z. F.; Jiang, Y.; Field, R. W. (Hg.) (2010): Fundamentals of Pressure-Driven Membrane Separation Processes. Online verfügbar unter www.sciencedirect.com/science/ article/pii/ B978185617632300001X.

17. Dang, Hai Quang; Price, William E.; Nghiem, Long Duc (2014): The effects of feed solution temperature on pore size and trace organic contaminant rejection by the nanofiltration membrane NF270. In: *Separation and Purification Technology* 125, S. 43–51. DOI: 10.1016/j.seppur .2013.12.043.

18. Darwish, M. A.; Abdulrahim, H. K.; Hassan, A. S.; Mabrouk, A. A.; Sharif, A. O. (2014): The forward osmosis and desalination. In: *Desalination and Water Treatment*, S. 1–27. DOI: 10.1080/19443994.2014.995140.

19. Dey, Pinaki; Linnanen, Lassi; Pal, Parimal (2012): Separation of lactic acid from fermentation broth by cross flow nanofiltration: Membrane characterization and transport modelling. In: *Desalination* 288, S. 47–57. DOI: 10.1016/j.desal.2011.12.009.

20. Din, Nur Akmal Solehah; Lim, Seng Joe; Maskat, Mohamad Yusof; Mutalib, Sahilah Abd; Zaini, Nurul Aqilah Mohd (2021): Lactic acid separation and recovery from fermentation broth by ion-exchange resin: A review. In: *Bioresour. Bioprocess.* 8 (1). DOI: 10.1186/s40643-021-00384-4.

21. Dr. Scott Chalmers (1998): Interference-based measurement of semi-transparent thin film thickness, OP-R: Optical Thin Film Measurement, Version: Fall 99.

22. Dutta, K.; Mahanty, B.; Daverey, A.; Sundari, I. S.; Sen, S. (2016): Biorefinery and Possible Negative Impacts on the Food Market.

23. Ecker, J.; Raab, T.; Harasek, M. (2012): Nanofiltration as key technology for the separation of LA and AA. In: *Journal of Membrane Science* 389, S. 389–398. DOI: 10.1016/ j.memsci.2011.11.004.

24. Eş, Ismail; Mousavi Khaneghah, Amin; Barba, Francisco J.; Saraiva, Jorge A.; Sant'Ana, Anderson S.; Hashemi, Seyed Mohammad Bagher (2018): Recent advancements in lactic acid production - a review. In: *Food research international (Ottawa, Ont.)* 107, S. 763–770. DOI: 10.1016/j.foodres.2018.01.001.

25. Finch, H.J.S.; Samuel, A. M.; Lane, G.P.F. (2014): Conservation of grass and forage crops. In:, S. 513–526.

26. Franco, Marcia; Hurme, Timo; Winquist, Erika; Rinne, Marketta (2019): Grass silage for biorefinery—A meta-analysis of silage factors affecting liquid–solid separation. In: *Grass Forage Sci* 74 (2), S. 218–230. DOI: 10.1111/gfs.12421.

27. Garedew, Mahlet; Lin, Fang; Song, Bing; DeWinter, Tamara M.; Jackson, James E.; Saffron, Christopher M. et al. (2020): Greener Routes to Biomass Waste Valorization: Lignin Transformation Through Electrocatalysis for Renewable Chemicals and Fuels Production. In: *ChemSusChem* 13 (17), S. 4214–4237. DOI: 10.1002/cssc.202000987.

28. González, M. Isabel; Alvarez, Silvia; Riera, Francisco A.; Álvarez, Ricardo (2008): Lactic acid recovery from whey ultrafiltrate fermentation broths and artificial solutions by nanofiltration. In: *Desalination* 228 (1-3), S. 84–96. DOI: 10.1016/j.desal.2007.08.009.

29. Grand view Research. (2021): Lactic Acid Market Share | Industry Report, 2021-2028. (2021, April). Lactic Acid Market Share | Industry Report, 2021-2028. Online verfügbar unter https://www.grandviewresearch.com/industry-analysis/lactic-acid-and-poly-lactic-acid-market.

30. Haag, Nicola Leonard; Grumaz, Christian; Wiese, Franziska; Kirstahler, Philipp; Merkle, Wolfgang; Nägele, Hans-Joachim et al. (2016): Advanced green biorefining: effects of ensiling treatments on lactic acid production, microbial activity and supplementary methane formation of grass and rye. In: *Biomass Conv. Bioref.* 6 (2), S. 197–208. DOI: 10.1007/s13399-015-0178-2.

31. J. Ecker; M. Schaffenberger; W. Koschuh; M. Mandl; H.G. Böchzelt; H. Schnitzer et al. (2012): Green Biorefinery Upper Austria – Pilot Plant operation,Separation and Purification Technology, Volume 96,2012.

32. Joglekar, H. G.; Rahman, Imran; Babu, Suresh; Kulkarni, B. D.; Joshi, Ajit (2006): Comparative assessment of downstream processing options for lactic acid. In: *Separation and Purification Technology* 52 (1), S. 1–17. DOI: 10.1016/j.seppur.2006.03.015.

33. Komesu, Andrea; Wolf Maciel, Maria Regina; Maciel Filho, Rubens (2017): Separation and Purification Technologies for Lactic Acid – A Brief Review. In: *BioResources* 12 (3). DOI: 10.15376/biores.12.3.6885-6901.

34. Krishna, Battula; K.V, Narayana Saibaba; Gantala, Sarva Sai Nikhilesh; Tarun, Besetty (2019): Industrial production of lactic acid and its applications 1, S. 42–54.

35. Kromus, Stefan; Wachter, B.; Koschuh, Werner; Mandl, M.; Krotscheck, Christian; Narodoslawsky, Michael (2004): The Green Biorefinery Austria - Developement of an Integrated System for Green Mass Utilization. In: *Nature* 18.

36. Kumar, Anil; Thakur, Avinash; Panesar, Parmjit Singh (2019): Lactic acid and its separation and purification techniques: A review. In: *Rev Environ Sci Biotechnol* 18 (4), S. 823–853. DOI: 10.1007/s11157-019-09517-w.

37. Lei Yao; Zhen Qin; Qiming Chen; Mengyao Zhao; Hefei Zhao; Waheed Ahmad et al. (2018): Insights into the nanofiltration separation mechanism of monosaccharides by molecular dynamics simulation.

38. Li, Chenglong; Gao, Ming; Zhu, Wenbin; Wang, Nuohan; Ma, Xiaoyu; Wu, Chuanfu; Wang, Qunhui (2021): Recent advances in the separation and purification of lactic acid from fermentation broth. In: *Process Biochemistry* 104, S. 142–151. DOI: 10 .1016/ j.procbio . 2021.03.011.

39. Melin, Thomas; Rautenbach, R. (Hg.) (2007): Membranverfahren. Grundlagen der Modul- und Anlagenauslegung. 3., aktualisierte und erw. Aufl. Berlin, New York: Springer (Chemische Technik/Verfahrenstechnik).

40. Meng, Kexin; Zhang, Guangyu; Ding, Chuanqin; Zhang, Tongyang; Yan, Hui; Zhang, Dongpei et al. (2020): Recent Advances on Purification of Lactic Acid. In: *Chemical record (New York, N.Y.)* 20 (11), S. 1236–1256. DOI: 10.1002/tcr.202000055.

41. Muck, R. E.; Kung, Limin (2007): Silage production. In: *Forages: The Science of Grassland Agriculture* 2.

42. Nanda, Dipankar; Tung, Kuo-Lun; Li, Yu-Ling; Lin, Nien-Jung; Chuang, Ching-Jung (2010): Effect of pH on membrane morphology, fouling potential, and filtration performance of nanofiltration membrane for water softening. In: *Journal of Membrane Science* 349 (1-2), S. 411–420. DOI: 10.1016/j.memsci.2009.12.004.

43. Pachapur, V. L.; Sarma, S. J.; Brar, S. K.; Chaabouni, E.2016 (2016): Platform Chemicals, S. 1–20. DOI: 10.1016/B978-0-12-802980-0.00001-8.

44. Phanthumchinda, Natnirin; Thitiprasert, Sitanan; Tanasupawat, Somboon; Assabumrungrat, Suttichai; Thongchul, Nuttha (2018): Process and cost modeling of lactic acid recovery from fermentation broths by membrane-based process. In: *Process Biochemistry* 68, S. 205–213. DOI: 10.1016/j.procbio.2018.02.013.

45. Pleissner, Daniel; Schneider, Roland; Venus, Joachim; Koch, Timo (2017): Separation of lactic acid and recovery of salt-ions from fermentation broth. In: *J. Chem. Technol. Biotechnol* 92 (3), S. 504–511. DOI: 10.1002/jctb.5023.

46. Purkait, Mihir K.; Singh, Randeep (2018): Membrane technology in separation science. Boca Raton: Taylor & Francis.

47. Rodrigues, C.; Vandenberghe, L.P.S.; Woiciechowski, A. L.; Oliveira, J. de; Letti, L.A.J.; Soccol, C. R. (2017): Production and Application of Lactic Acid.

48. S.J. Sarma; M. Ayadi; S.K. Brar (2016): Chapter 2 - Biorefinery: General Overview. In: Satinder Kaur Brar, Saurabh Jyoti Sarma und Kannan Pakshirajan (Hg.): Platform Chemical Biorefinery. Amsterdam:Elsevier,S.21–32.Online verfügbar unter https: // www.sciencedirect.com/science/article/pii/B978012802980000002X.

49. Singh, Rajindar (2015): Chapter 1 - Introduction to Membrane Technology. Second Edition. Online verfügbar unter www.sciencedirect.com/science/article/pii/B978044463362000001X.

50. Tewari, P. K. (2015): Nanocomposite Membrane Technology: Fundamentals & Applications.

51. Uragami, Tadashi (2017): Science and technology of separation membranes. Chichester West Sussex UK, Hoboken NJ USA: Wiley.

52. Verliefde, Arne R. D.; Cornelissen, Emile R.; Heijman, Sebastiaan G. J.; Hoek, Eric M. V.; Amy, Gary L.; van der Bruggen, Bart; van Dijkt, Johannis C. (2009): Influence of solute-membrane affinity on rejection of uncharged organic solutes by nanofiltration membranes. In: *Environmental science & technology* 43 (7), S. 2400–2406. DOI: 10.1021/es803146r.

53. Vertès, Alain A.; Qureshi, Nasib; Blaschek, Hans P.; Yukawa, Hideaki (Hg.) (2020): Green Energy to Sustainability. Strategies for global industries. Hoboken, NJ: Wiley. Online verfügbar unter https://onlinelibrary.wiley.com/doi/book/10.1002/9781119152057.

54. Weng, Yu-Hsiang; Wei, Hwa-Jou; Tsai, Tsung-Yen; Chen, Wei-Hsi; Wei, Tsong-Yang; Hwang, Wen-Song et al. (2009): Separation of acetic acid from xylose by nanofiltration. In: *Separation and Purification Technology* 67 (1), S. 95–102. DOI: 10.1016/j.seppur.2009.03.030.

55. World Meteorological Organization. 2021: Group, P. (n.d.). United In Science 2021 | E-Library. https://library.wmo.int/index.php?lvl=notice_display&id=21946#.YcSPQWjMLIW. Online verfügbar unter https://library.wmo.int/index.php?lvl=notice_display&id=21946#.YcSPQWjMLIW.

56. Xiao, L.-S. (Hg.) (2017): Membrane-Based Separation. Online verfügbar unter www.sciencedirect.com/science/article/pii/B9780128034101000025.

57. Yang, Shang-Tian; El-Enshasy, Hesham A.; Thongchul, Nuttha (Hg.) (2013): Bioprocessing technologies in biorefinery for sustainable production of fuels, chemicals, and polymers. Hoboken, New Jersey: Wiley.